DEPARTMENT OF COMMERCE
LUTHER H. HODGES, Secretary

WEATHER BUREAU
F. W. REICHELDERFER, Chief

MONTHLY WEATHER REVIEW

JAMES E. CASKEY, JR., Editor

Volume 89
Number 4

APRIL 1961

Closed March 15, 1961
Issued April 15, 1961

THE REDUCTION OF TRUNCATION ERROR BY EXTRAPOLATION TECHNIQUES [1]

W. LAWRENCE GATES

University of California, Los Angeles, Calif.
[Manuscript received December 5, 1961]

ABSTRACT

By the use of two separate mesh sizes instead of one in computing finite differences, an extrapolation to effective "zero" mesh size may be made in order to reduce the truncation error, as originally suggested by Richardson. This technique of "difference extrapolation" is applied to the estimation of individual differentials in the barotropic vorticity equation, and here corresponds to the use of "second-order" finite differences. The truncation-induced phase speed lag of the difference solution relative to the true solution is shown to be systematically reduced, especially for the shorter waves. Next, the extrapolation is applied with two separate solutions of the barotropic difference equation, with the result that the phase speeds are further improved, but at the expense of an amplitude distortion of about 10 percent. This amplitude distortion may be removed for a particular wavelength, and a small further phase speed improvement obtained, but the amplitude distortion remains for other wavelengths. These methods of "solution extrapolation" are therefore felt to be unsuitable for routine use. The method of "difference extrapolation," however, preserves the solution's amplitude, and if used in conjunction with a suitable smoothing procedure should result in a net error reduction for those waves resolved by the mesh and retained by the smoothing.

1. INTRODUCTION

In the approximation of spatial derivatives by finite differences, a truncation error is made which in general depends upon the size of the finite space increment, as well as upon the wavelength and orientation of the continuous field being estimated. The most widely-used procedure is the familiar centered space difference, which we may illustrate in the case of the first derivative of a (continuous) function f as

$$\frac{\partial f}{\partial x} \simeq \Delta f \equiv \frac{f(x+\Delta x)-f(x-\Delta x)}{2\Delta x}, \tag{1}$$

where x is a typical space coordinate and Δx is the mesh size. The error of this approximation is easily shown to be of the order $(\Delta x)^2$, i.e.,

$$e(f) \equiv \Delta f - \frac{\partial f}{\partial x} = O(\Delta x^2). \tag{2}$$

This approximation is furthermore a consistent one in the sense that $e(f) \to 0$ as $\Delta x \to 0$. It is the purpose of this study to utilize such Δx-dependence of the truncation error in order to improve the accuracy of the finite-difference approximation itself, using an extrapolation technique. The procedure to be described will be seen to be related to several proposed methods for the reduction of truncation error and for smoothing.

2. THE EXTRAPOLATION TECHNIQUE

Since the accuracy of the difference approximation depends upon the mesh spacing, it occurs to one that from, say, *two* finite difference estimates, made with different grid increments, an improved estimate of the derivative might be made. Considering the estimation of $\partial f/\partial x$ for

[1] This research has been supported by the Geophysics Research Directorate of the Air Force Cambridge Research Center under contract No. AF 19(604)-4965.

example, and denoting the two grid increments by Δx_1, and Δx_2, we have

$$(\Delta f)_{1,2}=\frac{f(x+\Delta x_{1,2})-f(x-\Delta x_{1,2})}{2\Delta x_{1,2}}, \tag{3}$$

where $(\Delta f)_{1,2}$ denotes either of the two difference estimates of $\partial f/\partial x$. Since the error of $(\Delta f)_{1,2}$ is of the order $(\Delta x)^2$, we may extrapolate to an effective zero mesh size by forming the linear combination

$$(\Delta f)_0=\frac{\rho^2(\Delta f)_1-(\Delta f)_2}{\rho^2-1}, \tag{4}$$

where $\rho=\Delta x_2/\Delta x_1>1$. This "extrapolation to the limit" is illustrated in figure 1, and was evidently first suggested by Richardson [6].

In order to show that the estimate (4) is a systematic improvement over either $(\Delta f)_1$ or $(\Delta f)_2$ alone, we may expand f in a Taylor series with remainder about $x=0$,

$$f(x\pm\Delta x_1)=f(x)\pm\Delta x_1\frac{\partial f}{\partial x}+\frac{\Delta x_1^2}{2}\frac{\partial^2 f}{\partial x^2}\pm\frac{\Delta x_1^3}{6}\frac{\partial^3 f}{\partial x^3}+\frac{\Delta x_1^4}{24}\frac{\partial^4 f}{\partial x^4}\pm\frac{\Delta x_1^5}{120}\left(\frac{\partial^5 f}{\partial x^5}\right)_{\theta_1,\theta_2}, \tag{5}$$

$$f(x\pm\Delta x_2)=f(x\pm\rho\,\Delta x_1)=f(x)\pm\rho\,\Delta x_1\frac{\partial f}{\partial x}+\frac{\rho^2\Delta x_1^2}{2}\frac{\partial^2 f}{\partial x^2}\pm\frac{\rho^3\Delta x_1^3}{6}\frac{\partial^3 f}{\partial x^3}+\frac{\rho^4\Delta x_1^4}{24}\frac{\partial^4 f}{\partial x^4}\pm\frac{\rho^5\Delta x_1^5}{120}\left(\frac{\partial^5 f}{\partial x^5}\right)_{\theta_3,\theta_4}, \tag{6}$$

where $\theta_1, \ldots, \theta_4$ are suitable points in the vicinity of the origin. Inserting these expressions into (3) and (4), we find the truncation error

$$e(f)=(\Delta f)_0-\frac{\partial f}{\partial x}=O(\Delta x^4). \tag{7}$$

This result was only to be expected, however, since the ρ^2-extrapolation in (4) was designed to eliminate the dominant $(\Delta x)^2$ error-dependence of $(\Delta f)_{1,2}$.

This extrapolation technique has been used with some success in steady-state problems of engineering (Salvadori [8]), and is a relatively well-known procedure in the numerical analysis of linear differential equations (see, for example, Buckingham [1] or Hartree [3]). In the nonlinear, time-dependent equations typical of dynamical weather prediction, however, we have no guarantee that its use will result in a systematic improvement. In the first place, the extrapolation might be performed at each time step in the calculation of the non-homogeneous terms, or might be applied to the entire solutions from the separate grids. Moreover, in the presence of several wavelengths in the field of the dependent variable, the extrapolation may improve the difference estimates for only certain waves and fail to provide an overall error reduction of the order implied by (7). In spite of these misgivings, it seems worthwhile to give the extrapolation technique some further consideration, particularly in view of its relations to other computational schemes discussed below.

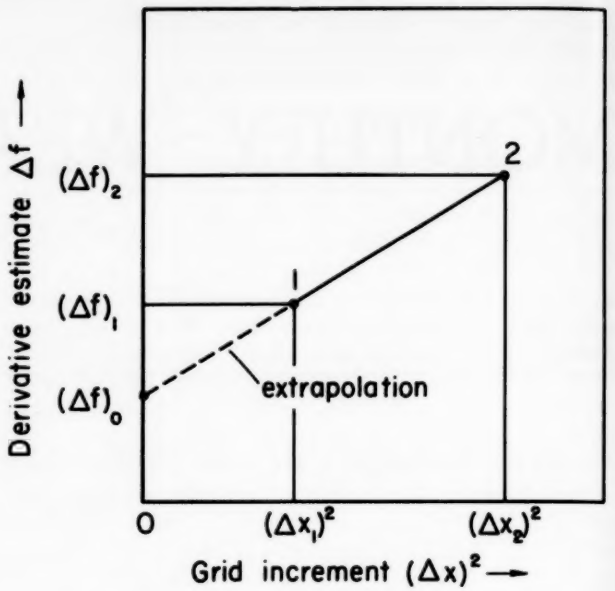

FIGURE 1.—The Richardson extrapolation technique for the reduction of truncation error, applied to the calculation of the derivative $\partial f/\partial x$ by centered differences.

For the sake of clarity, let us select $\Delta x_2/\Delta x_1=2$, and again consider the estimation of $\partial f/\partial x$ by centered differences. Expanding (4) we find, with $\rho^2=4$,

$$(\Delta f)_0=\frac{4}{3}(\Delta f)_1-\frac{1}{3}(\Delta f)_2, \tag{8}$$

which, upon use of (3), in turn yields

$$(\Delta f)_0=\frac{1}{12\Delta x_1}(f_{-2\Delta x}-8f_{-\Delta x}+8f_{\Delta x}-f_{2\Delta x}), \tag{9}$$

where $f_{-2\Delta x}$ denotes $f(x-2\Delta x)$, etc. This expression is recognized as just the "five-point" approximation to the first derivative.

The extrapolation technique may also be employed in the estimation of other differentials, of which the familiar Laplacian $\nabla^2 f$ is a convenient example. Proceeding as before, we find

$$(\Delta^2 f)_0=\frac{\rho^2(\Delta^2 f)_1-(\Delta^2 f)_2}{\rho^2-1}, \tag{10}$$

where $(\Delta^2 f)_{1,2}$ are the difference estimates of $\nabla^2 f$ with a truncation error $O(\Delta x^2)$. The error of the extrapolated estimate $(\Delta^2 f)_0$ is now $O(\Delta x^4)$. If we select $\rho^2=2$, we then have simply

$$(\Delta^2 f)_0=2(\Delta^2 f)_1-(\Delta^2 f)_2. \tag{11}$$

This formula is the same as that found by Knighting [4] in considering both the conventional five-point Laplacian estimate and that involving the four "corner" points at a distance $\sqrt{2}$ greater from the central point. This scheme is generated by a 45° rotation of the grid axes, and is an improvement on the directionally-averaged estimate of the Laplacian proposed by Thompson [10].

As a final case of meteorological interest, we note that the extrapolation method may be used in estimating the Jacobian $J(a, b)$ of two scalar variables a and b. The conventional estimate

$$I_1(a,b)=(4\Delta x_1^2)^{-1}[(a_{i+1,j}-a_{i-1,j})(b_{i,j+1}-b_{i,j-1}) -(a_{i,j+1}-a_{i,j-1})(b_{i+1,j}-b_{i-1,j})] \quad (12)$$

may be combined with the analogous estimate with Δx_2, yielding

$$I_0(a,b)=[\rho^2 I_1(a,b)-I_2(a,b)][\rho^2-1]^{-1}, \quad (13)$$

since the dominant truncation error in each case is $O(\Delta x^2)$. The error of the estimate $I_0(a,b)$ is readily shown to be $O(\Delta x^4)$, and hence a systematic improvement over either $I_1(a,b)$ or $I_2(a,b)$ alone. If we select $\rho=2$ as before, we find

$$I_0(a,b)=2I_1(a,b)-I_2(a,b) \quad (14)$$

which has also been suggested by Knighting [4] using the 45° "rotated" axes for $I_2(a,b)$. Knighting, Jones, and Hinds [5] have used both $I_1(a,b)$ and $I_2(a,b)$ as *separate* estimates of the Jacobian in numerical integration of a simple dynamical model, and find in general that the "rotated" axes estimate ($I_2(a,b)$) yields a smoother field, and in some cases improved the prediction. From the present viewpoint it would have been interesting if *both* estimates were used as in (14).

3. THE EXTRAPOLATION OF DIFFERENTIALS IN THE BAROTROPIC VORTICITY EQUATION

Instead of the estimation of a single differential, the meteorological prediction problem involves the solution of a complete differential equation. The simplest of such equations is that of the linearized barotropic model,

$$\frac{\partial^3\psi}{\partial t\partial x^2}+U\frac{\partial^3\psi}{\partial x^3}+\beta\frac{\partial\psi}{\partial x}=0, \quad (15)$$

where ψ is the stream function of the nondivergent flow, U the assumed constant zonal current, β the Rossby parameter, and x and t the eastward spatial and time coordinates, respectively. As noted earlier, there are evidently two ways of applying the Richardson extrapolation technique: Either to improve the estimates of each differential of (15) separately, or to improve the solution by a suitable combination of two solutions found with different mesh sizes. We shall consider both methods in this and the following sections.

The first extrapolation method, which might be termed "extrapolation of differentials," is based upon the fact that the truncation error of $\partial\psi/\partial x$, $\partial^2\psi/\partial x^2$, and $\partial^3\psi/\partial x^3$ is $O(\Delta x^2)$ when the usual centered space differences are used. The use of centered time differences in the solution, however, introduces some awkwardness into the analysis by virtue of its inapplicability for the first time step. Forward time differences, on the other hand, are unstable and consequently unsuitable. There remains the method of implicit differences (Gates [2]), and it will be used here in order to simplify the analysis and at the same time to employ a method applicable in practice.

The essence of the implicit difference approximation is the use of information at *both* the current discrete time step τ and at the next time step $\tau+1$ in order to evaluate centered spatial differences. For the derivative $\partial\psi/\partial x$ we thus have

$$\frac{\partial\psi}{\partial x}\simeq\frac{1}{2}((\Delta f)_\tau+(\Delta f)_{\tau+1}), \quad (16)$$

where Δf denotes the usual centered difference estimate as in (3). If both $(\Delta f)_\tau$ and $(\Delta f)_{\tau+1}$ are now improved by the extrapolation technique with $\rho^2=\Delta x_2/\Delta x_1=4$ for convenience, we have

$$\frac{\partial\psi}{\partial x}\simeq(24\Delta x_1)^{-1}[8(\psi_{m+1,\tau+1}-\psi_{m-1,\tau+1}+\psi_{m+1,\tau}-\psi_{m-1,\tau}) -(\psi_{m+2,\tau+1}-\psi_{m-2,\tau+1}+\psi_{m+2,\tau}-\psi_{m-2,\tau})], \quad (17)$$

where

$$\psi_{m,\tau}=\psi(m\Delta x,\tau\Delta t),\ m=0,\pm1,\ldots,\ \tau=0,1,\ldots.$$

In a similar manner we find the extrapolated implicit difference estimates

$$\frac{\partial^2\psi}{\partial x^2}\simeq(24\Delta x_1^2)^{-1}[16(\psi_{m+1,\tau+1}+\psi_{m-1,\tau+1}-2\psi_{m,\tau+1}+\psi_{m+1,\tau} +\psi_{m-1,\tau}-2\psi_{m,\tau})-(\psi_{m+2,\tau+1}+\psi_{m-2,\tau+1} -2\psi_{m,\tau+1}+\psi_{m+2,\tau}+\psi_{m-2,\tau}-2\psi_{m,\tau})], \quad (18)$$

$$\frac{\partial^3\psi}{\partial x^3}\simeq(96\Delta x_1^3)^{-1}[32(\psi_{m+2,\tau+1}-2\psi_{m+1,\tau+1}+2\psi_{m-1,\tau+1} -\psi_{m-2,\tau+1}+\psi_{m-2,\tau}-2\psi_{m+1,\tau}+2\psi_{m-1,\tau}-\psi_{m-2,\tau}) -(\psi_{m+4,\tau+1}-2\psi_{m+2,\tau+1}+2\psi_{m-2,\tau+1}-\psi_{m-4,\tau+1} +\psi_{m+4,\tau}-2\psi_{m+2,\tau}+2\psi_{m-2,\tau}-\psi_{m-4,\tau})], \quad (19)$$

$$\frac{\partial^3\psi}{\partial t\partial x^2}\simeq(12\Delta t\Delta x_1^2)^{-1}[16(\psi_{m+1,\tau+1}+\psi_{m-1,\tau+1}-2\psi_{m,\tau+1} -\psi_{m+1,\tau}-\psi_{m-1,\tau}+2\psi_{m,\tau})-(\psi_{m+2,\tau+1}+\psi_{m-2,\tau+1} -2\psi_{m,\tau+1}-\psi_{m+2,\tau}-\psi_{m-2,\tau}+2\psi_{m,\tau})]. \quad (20)$$

Inserting these expressions into (15) and assuming a solution of the form $\psi_{m,\tau}=A(\tau)e^{im\alpha}$, where $\alpha=2\pi\Delta x/L$ with L the wavelength, we find after some manipulation

$$(a+ib)A(\tau+1)-(a-ib)A(\tau)=0, \quad (21)$$

where

$$a=\cos\alpha-7, \quad (22)$$

$$b=\frac{\Delta t \sin\alpha}{2\Delta x_1}\left[U(\cos^2\alpha+\cos\alpha-8)+\beta\Delta x_1^2\left(\frac{\cos\alpha-4}{\cos\alpha-1}\right)\right]. \quad (23)$$

The so-called amplification matrix of (21) is given by

$$G=\frac{a-ib}{a+ib}, \quad (24)$$

from which we see that $|G|^{1/2}=1$, a characteristic of the (stable) implicit difference scheme. The solution of (21) for arbitrary $t=\tau\Delta t$ may now be written as

$$A(\tau)=\Psi G^{\tau}, \quad (25)$$

where Ψ is the amplitude of the assumed initial condition $\psi_{m,0}=\Psi e^{im\alpha}$; i.e., $A(0)=\Psi$. From (25) we may then write the complete solution as

$$\psi_{m,\tau}=\Psi|G|^{\tau/2}\exp\{i[m\alpha+\tau\tan^{-1}(2ab/a^2-b^2)]\}. \quad (26)$$

Recalling $|G|^{1/2}=1$ and after some further manipulation, we may write this solution as

$$\psi_{m,\tau}=\Psi\exp\{i[m\alpha-\tau\tan^{-1}(4\lambda^*/4-\lambda^{*2})]\}, \quad (27)$$

where

$$\lambda^*=\frac{\Delta t}{\Delta x_1}\sin\alpha\left\{U\left[\frac{\cos^2\alpha+\cos\alpha-8}{\cos\alpha-7}\right]-\frac{\beta L^2/4\pi^2}{\left(\frac{\sin\alpha/2}{\alpha/2}\right)^2}\left[\frac{2\cos\alpha-8}{\cos\alpha-7}\right]\right\}. \quad (28)$$

Comparing λ^* with the corresponding parameter

$$\lambda=\frac{\Delta t}{\Delta x}\sin\alpha\left[U-\frac{\beta L^2/4\pi^2}{\left(\frac{\sin\alpha/2}{\alpha/2}\right)^2}\right] \quad (29)$$

occurring in the implicit difference solution of the barotropic vorticity equation without extrapolation (Gates [2]), we note that they differ only by the presence of the bracketed terms of (28). The variation of λ^* with L and Δx_1 is shown in figure 2 for the selected values $\Delta t=1$ hr., $U=20$ m. sec.$^{-1}$, and $\beta(45°\text{ lat.})=1.619\times10^{-13}$ cm.$^{-1}$ sec.$^{-1}$ By comparison with the corresponding values of λ also given, we note $\lambda^*\geq\lambda$ for all Δx and L.

The solutions with and without extrapolation may now be conveniently compared by writing (27) in the form

$$\psi_{m,\tau}=\Psi\exp\{ik[m\Delta x_1-\tau\Delta t C_N^*]\}, \quad (30)$$

where C_N^* is the phase speed of the numerical solution and $k=2\pi/L$ is the wave number. Here C_N^* is given by

$$C_N^*=\frac{L}{2\pi\Delta t}\tan^{-1}\left(\frac{4\lambda^*}{4-\lambda^{*2}}\right), \quad (31)$$

and its variation with Δx and L is shown in figure 3, along with the corresponding data for C_N without extrapolation. The phase speeds are seen to be systematically increased for all L and Δx, particularly in the intermediate cases, say $5\Delta x\leq L\leq10\Delta x$. If we compare these curves with the corresponding Rossby phase speed

$$C_R=U-\frac{\beta L^2}{4\pi^2} \quad (32)$$

of the analytic solution of (15), we may say that the phase speed error of the numerical solution is approximately halved by the use of the Richardson extrapolation technique with $\rho=2$.

The departure of the numerical phase speeds from the corresponding Rossby phase speeds of the continuous solution is due to both space and time truncation errors. The present extrapolation technique, we note, seeks to reduce only the spatially induced error, and it is therefore of interest to investigate its relative efficiency in comparison to the limiting case of $\Delta x\to0$. From (28) we first see that

$$\lim_{\Delta x\to0}\lambda^*=\frac{2\pi\Delta t}{L}C_R, \quad (33)$$

where C_R is given by (32). Hence, from (31) we have

$$\lim_{\Delta x\to0}C_N^*=\frac{L}{2\pi\Delta t}\tan^{-1}\left[\frac{2\pi\Delta t\,C_R/L}{1-(\pi\Delta t\,C_R/L)^2}\right], \quad (34)$$

and the difference between this expression and C_R may then be attributed to the time truncation error alone.[2] In other words, the limiting speeds given by (34), and shown in figure 3, are the most accurate which could be found by reduction of the space mesh alone, and are a reasonable basis for comparison with the results of the extrapolation technique. In the case of $\Delta x_1=100$ km., for example, we see that as L increases an increasingly large fraction of the total possible phase speed improvement is provided by the present extrapolation. We also note that for $L>1500$ km. (with the assumed values of Δt, U, and β) the limiting phase speed need not be distinguished from C_R; this is to say that the time truncation affects mainly the shorter waves.

4. THE EXTRAPOLATION OF SOLUTIONS OF THE BAROTROPIC VORTICITY EQUATION

In the earlier discussion of the extrapolation technique, we noted that the method may evidently be applied either in the estimation of the individual differentials or in the improvement of the separate solutions themselves. The first method was considered in section 3 above, and we now turn our attention to the second approach, which may be termed "extrapolation of solutions." This technique is, in fact, that originally suggested by Richardson [6], who termed it the "deferred approach to the limit."

Continuing to use implicit differences for convenience, the difference equation approximating (15) is

[2] This same limiting expression also results from the unextrapolated solutions given by Gates [2].

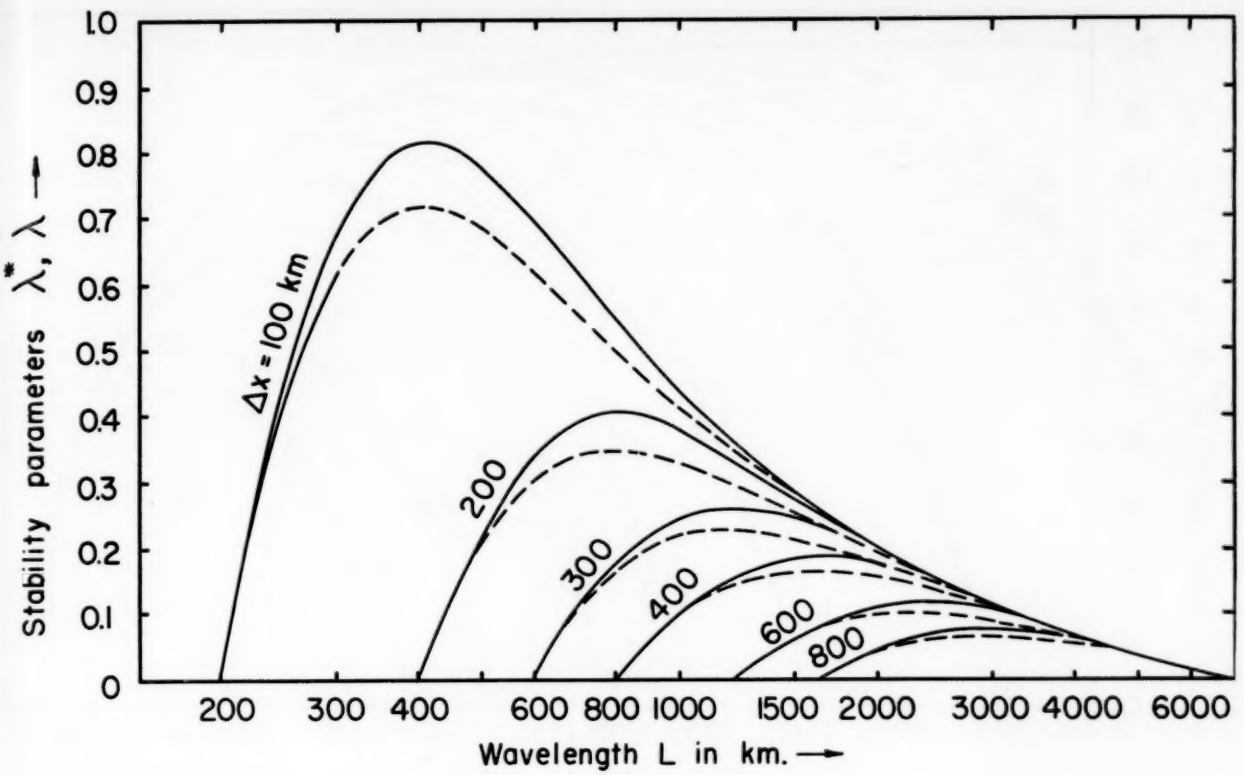

FIGURE 2.—The variation of the parameter λ^* of (28) with Δx and L. Also shown by the dashed lines is the corresponding parameter (29) for the unextrapolated difference case. Here $\Delta t=1$ hr., $U=20$ m.sec.$^{-1}$, and $\beta\ (45^\circ)=1.619\times10^{-13}$ cm.$^{-1}$ sec.$^{-1}$

$$(\Delta t\Delta x^2)^{-1}(\psi_{m+1,\tau+1}-2\psi_{m,\tau+1}+\psi_{m-1,\tau+1}-\psi_{m+1,\tau}+2\psi_{m,\tau}-\psi_{m-1,\tau})+U(4\Delta x^3)^{-1}(\psi_{m+2,\tau}-2\psi_{m+1,\tau}+2\psi_{m-1,\tau}-\psi_{m-2,\tau}+\psi_{m+2,\tau+1}-2\psi_{m+1,\tau+1}+2\psi_{m-1,\tau+1}-\psi_{m-2,\tau+1})+\beta(4\Delta x)^{-1}(\psi_{m+1,\tau}-\psi_{m-1,\tau}+\psi_{m+1,\tau+1}-\psi_{m-1,\tau+1})=0. \quad (35)$$

The solution of this equation for the simple harmonic initial conditions used earlier is readily shown to be

$$\psi_{m,\tau}=\Psi\exp\left\{i\left[m\alpha-\tau\tan^{-1}\left(\frac{4\lambda}{4-\lambda^2}\right)\right]\right\}, \quad (36)$$

where λ is given by (29) and $\alpha=2\pi\Delta x/L$ as before.

We may now write this solution specifically for our two mesh sizes Δx_1 and Δx_2 as

$$\psi_{m_1,\tau}=\Psi\exp\left\{i\left[m_1\alpha_1-\tau\tan^{-1}\left(\frac{4\lambda_1}{4-\lambda_1^2}\right)\right]\right\}, \quad (37)$$

and

$$\psi_{m_2,\tau}=\Psi\exp\left\{i\left[m_2\alpha_2-\tau\tan^{-1}\left(\frac{4\lambda_2}{4-\lambda_2^2}\right)\right]\right\}, \quad (38)$$

and seek to combine them by the extrapolation technique. Since the truncation error of both (37) and (38) is $O(\Delta x^2)$, the appropriate extrapolation is of the form

$$\psi'_{m,\tau}\equiv(\rho^2\psi_{m_1,\tau}-\psi_{m_2,\tau})(\rho^2-1)^{-1}. \quad (39)$$

Selecting $\rho=\Delta x_2/\Delta x_1=2$ for convenience, we then have

$$\psi'_{m,\tau}=\frac{4}{3}\psi_{m_1,\tau}-\frac{1}{3}\psi_{m_2,\tau}. \quad (40)$$

Combining the separate solutions (37) and (38) according to (40), and noting $m_1\alpha_1=m_2\alpha_2$ at the points of the larger mesh, we find after some manipulation

$$\psi'_{m_2,\tau}=\Psi A\exp\{ik[m_2\Delta x_2-\tau\Delta tC'_N]\}, \quad (41)$$

where the amplitude factor A is given by

$$A=\frac{1}{3}\left\{17-8\cos\left[\tau\tan^{-1}\left(\frac{4\lambda_1}{4-\lambda_1^2}\right)-\tau\tan^{-1}\left(\frac{4\lambda_2}{4-\lambda_2^2}\right)\right]\right\} \quad (42)$$

and the numerical phase speed C'_N is given by

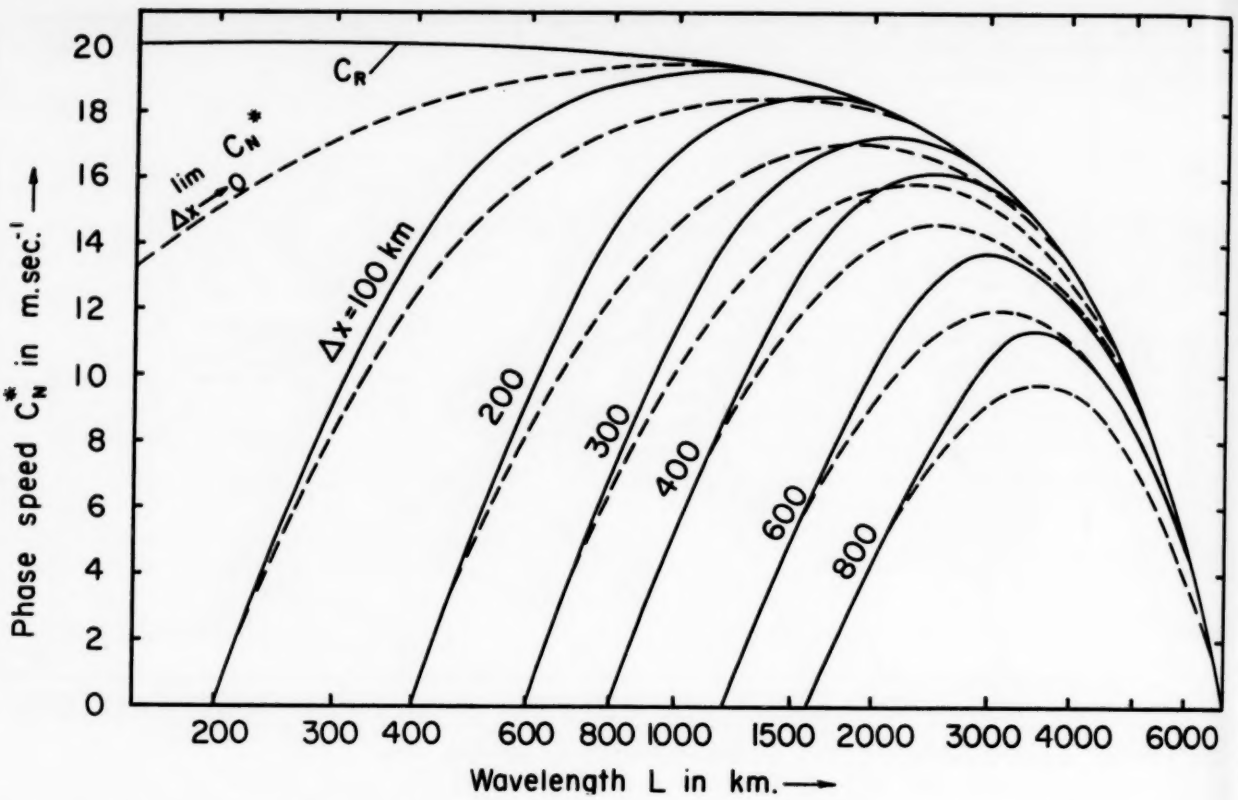

FIGURE 3.—The variation of the numerical phase speed C_N^* of (31) with Δx and L, for the "extrapolation of differences" technique. Also shown by the dashed lines is the corresponding phase speed for the unextrapolated difference case. The Rossby phase speed C_R of the continuous solution, and the limiting phase speed as $\Delta x \to 0$ are also given for comparison. Here $\Delta t = 1$ hr., $U = 20$ m. sec.$^{-1}$, and $\beta\ (45°) = 1.619 \times 10^{-13}$ cm.$^{-1}$ sec.$^{-1}$

$$C_N' = \frac{L}{2\pi\tau\Delta t} \tan^{-1} \left\{ \frac{4 \sin\left[\tau \tan^{-1}\left(\frac{4\lambda_1}{4-\lambda_1^2}\right)\right] - \sin\left[\tau \tan^{-1}\left(\frac{4\lambda_2}{4-\lambda_2^2}\right)\right]}{4 \cos\left[\tau \tan^{-1}\left(\frac{4\lambda_1}{4-\lambda_1^2}\right)\right] - \cos\left[\tau \tan^{-1}\left(\frac{4\lambda_2}{4-\lambda_2^2}\right)\right]} \right\}. \tag{43}$$

In order to simplify the further analysis of these results, let us assume that the extrapolation of the two solutions (40) is performed at each time step. It then suffices to examine the solution (41) for $\tau = 1$, and the amplitude factor and phase speed are accordingly simplified. If this is not done, and the extrapolation is considered to be applied after an arbitrary number of time steps τ, the amplitude A will vary with the choice of τ between the limits $1 \leq A \leq 5/3$.[3] With $\tau = 1$, the variation of A with Δx_1 and L is shown in table 1. We note that an amplitude distortion of a few percent of the extrapolated solution

[3] From the data presented by Gates [2], we may estimate that when $L = 1000$ km., $\Delta x_1 = 200$ km., $\Delta x_2 = 400$ km., $\Delta t = 1$ hr., $U = 20$ m. sec.$^{-1}$, and $\beta(45°) = 1.619 \times 10^{-13}$ cm.$^{-1}$ sec.$^{-1}$ the maximum amplitude (5/3) would first occur for $\tau \simeq 14$.

TABLE 1.—*The variation of the $\tau = 1$ amplitude distortion A of (42) as a function of wavelength L and selected mesh size Δx_1. Here the second mesh $\Delta x_2 = 2\Delta x_1$, $U = 20$ m. sec.$^{-1}$, $\Delta t = 1$ hr., and $\beta(45°) = 1.619 \times 10^{-13}$ cm.$^{-1}$ sec.$^{-1}$*

L (km.)	Grid mesh Δx_1, in km.			
	100	200	300	400
400	1.0066	----	----	----
600	1.0189	----	----	----
800	1.0044	1.0267	----	----
1000	1.0013	1.0114	*1.0117	----
1500	1.0001	1.0016	1.0050	†1.0052
2000	1.0000	1.0003	1.0013	1.0027
2500	1.0000	1.0001	1.0004	1.0009
3000	1.0000	1.0000	1.0001	1.0003
4000	1.0000	1.0000	1.0000	1.0001
6000	1.0000	1.0000	1.0000	1.0000

*for $L = 1200$ km.
†for $L = 1600$ km.

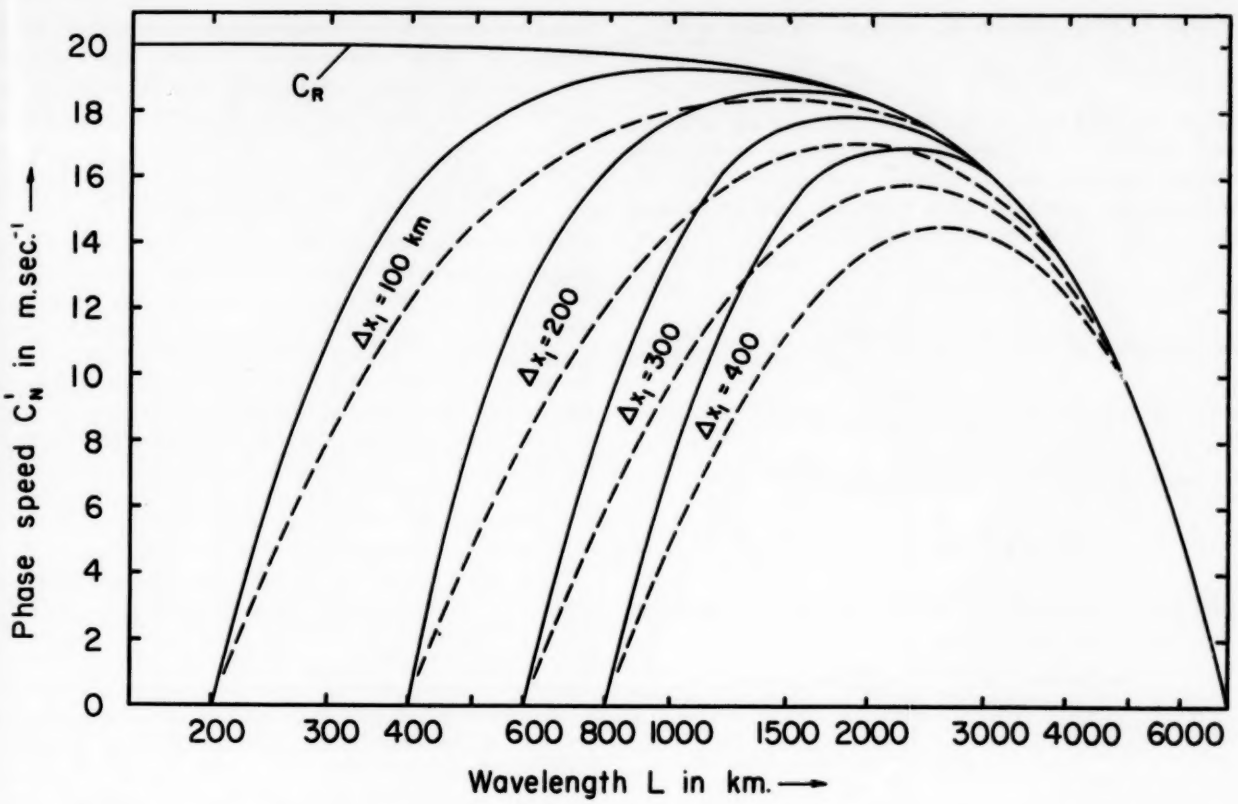

FIGURE 4.—The variation of the numerical phase speed C'_N of (43) with Δx_1 and L, for the "extrapolation of solutions" technique. Also shown by the dashed lines is the corresponding phase speed for the unextrapolated case. The Rossby phase speed C_R of the continuous solution is also given for comparison. Here $\Delta t = 1$ hr., $U = 20$ m. sec.$^{-1}$, and $\beta(45°) = 1.619 \times 10^{-13}$ cm.$^{-1}$ sec.$^{-1}$

(41) is confined to the shorter waves, for which the larger truncation errors are also made. For the longer wavelengths, $\lambda_1 \to \lambda_2$ and $A \to 1$.

The variation of the phase speed (43) of the extrapolated solution is shown in figure 4 for $\tau = 1$ as above. The phase speed improvement is seen to be most pronounced for the shorter waves; by comparison with figure 3 we note that approximately twice as much improvement over the unextrapolated solution is here obtained as was obtained by the technique of "extrapolation of differentials." For $\Delta x_1 = 100$ km., waves of length ≥ 1000 km. are now moved with very nearly the correct speed. The present method of "extrapolation of solutions" is therefore somewhat more effective than the method of section 3, at least as far as phase speeds are concerned.

5. A METHOD OF "OPTIMUM" EXTRAPOLATION

While the solution extrapolation technique described in the preceding section gives an overall improvement in phase speed, the small amplitude distortion also introduced (table 1) may be an undesirable feature for some purposes and accordingly may limit the practical application of the method. The solution extrapolation of (39) is based upon the elimination of the dominant spatial truncation error $O(\Delta x^2)$, and is in this sense only an approximation. It is possible to "extrapolate" the two solutions (37) and (38) in a slightly different way, and thereby to improve certain properties of the combined solution.

Let us form a simple linear combination of the solutions (37) and (38),

$$\psi''_{m,\tau} \equiv a\psi_{m_1,\tau} - b\psi_{m_2,\tau}, \tag{44}$$

where a and b are constants to be determined by the imposition of two conditions upon the solution $\psi''_{m,\tau}$. As a first condition, let us require the amplitude of $\psi''_{m,\tau}$ to equal Ψ, the amplitude of the initial conditions. This condition will then remove the amplitude factor A found in the previous method (at least for a certain wavelength, as discussed below). As a second condition, we may

require that the solution $\psi''_{m,\tau}$ move at the phase speed

$$C''_N=(\rho^2C_{N,1}-C_{N,2})(\rho^2-1)^{-1}, \tag{45}$$

where $C_{N,1}$ and $C_{N,2}$ are the phase speeds of the solutions (37) and (38). This condition is suggested by the more formal extrapolation technique, and insures that the solution $\psi''_{m,\tau}$ will move at a more accurate speed than does either of its component solutions. As before, let us select $\rho=2$, and note $m_1\alpha_1=m_2\alpha_2$. From these conditions we may then write (44) in the form

$$\begin{aligned}\psi''_{m,\tau}&=\Psi\exp\left\{i\left[m_2\alpha_2-\frac{4}{3}\tau\tan^{-1}\left(\frac{4\lambda_1}{4-\lambda_1^2}\right)\right.\right.\\&\qquad\left.\left.+\frac{1}{3}\tau\tan^{-1}\left(\frac{4\lambda_2}{4-\lambda_2^2}\right)\right]\right\}\\&=a\Psi\exp\left\{i\left[m_1\alpha_1-\tau\tan^{-1}\left(\frac{4\lambda_1}{4-\lambda_1^2}\right)\right]\right\}\\&\qquad-b\Psi\exp\left\{i\left[m_2\alpha_2-\tau\tan^{-1}\left(\frac{4\lambda_2}{4-\lambda_2^2}\right)\right]\right\},\end{aligned} \tag{46}$$

and thereby determine a and b. Setting $\tau=1$ as before and introducing the notation

$$\theta_1=\frac{1}{3}\tan^{-1}\left(\frac{4\lambda_1}{4-\lambda_1^2}\right), \tag{47}$$

$$\theta_2=\frac{1}{3}\tan^{-1}\left(\frac{4\lambda_2}{4-\lambda_2^2}\right) \tag{48}$$

for convenience, we find upon equating real and imaginary parts of each side of (46),

$$a=\frac{\sin[4(\theta_1-\theta_2)]}{\sin[3(\theta_1-\theta_2)]}, \tag{49}$$

$$b=\frac{\sin[\theta_1-\theta_2]}{\sin[3(\theta_1-\theta_2)]}. \tag{50}$$

For a selected Δx_1 and $\Delta x_2(=2\Delta x_1)$, the values of λ_1 and λ_2 vary with the wavelength L (see fig. 1). Hence θ_1 and θ_2 are likewise wavelength dependent, and it would appear that L must be specified for a unique determination of a and b. Fortunately, however, the values of a and b are not very sensitive to the value of L selected, as shown in table 2 below for the case $\Delta x_1=100$ km. For the longer wavelengths we notice that $a\to\frac{4}{3}$ and $b\to\frac{1}{3}$, corresponding to the extrapolation technique considered earlier in section 4. Since it is the shorter waves' phase speeds which require the most improvement, we may select $L=400$ km., the smallest permissible value (the resolution of the Δx_2 mesh). In this case, the phase speed of the solution $\psi''_{m,\tau}$,

$$C''_N=\frac{L}{2\pi\Delta t}\left[\frac{4}{3}\tan^{-1}\left(\frac{4\lambda_1}{4-\lambda_1^2}\right)-\frac{1}{3}\tan^{-1}\left(\frac{4\lambda_2}{4-\lambda_2^2}\right)\right], \tag{51}$$

varies as shown in figure 5. Here the corresponding phase speeds for the methods of sections 3 and 4, as well as that for the unextrapolated solution, are shown for comparison. We note that the use of $a=1.252$ and $b=0.358$ in (44) has given a small improvement over the use of $a=4/3$, and $b=1/3$ as in (40), which in turn is somewhat superior to the "extrapolation of differentials" of (27). This selection of a and b has, in effect, "tuned" the weighting scheme to give the greatest improvement at $L=400$ km., and is in this sense an "optimum' scheme. For other Δx_1, and a corresponding selection of a and b from table 2, generally similar results are obtained.

With this "tuning" to $L=400$ km., the amplitude is unity for this wavelength but is generally not unity for other wavelengths, as shown in table 3. This amplitude distortion, especially for the longer waves, greatly reduces the attractiveness of this "optimum" method, and is far more serious than that of the simpler method of "extrapolation of solutions" (39). The small phase speed improvement given by this method over that of (39) would therefore not be a useful improvement in practical application.

6. THE EXTRAPOLATION TECHNIQUE AND SMOOTHING

The basic extrapolation scheme (39) attempts to improve the accuracy of the finite-difference solutions by the removal of some of the spatial truncation error. Smoothing procedures (Shuman [9]), on the other hand, are designed to suppress the shorter waves (for which the larger truncation error is made) by the deliberate introduction of additional truncation, and in this sense the two procedures are opposed. If we write (39) for a discrete variable φ_m in the form

$$\varphi_{m_2}-\rho^2\varphi_{m_1}=(1-\rho^2)\varphi'_m, \tag{52}$$

where the notations are as before, and write Shuman's "three-point" smoothing operator for the same variable

TABLE 2.—*The variation of the weighting coefficients a and b of (44) with wavelength, for the case $\Delta x_1=100$ km., $U=20$ m. sec.$^{-1}$, $\rho=2$, $\Delta t=1$ hr., β (45°) $=1.619\times10^{-13}$ cm.$^{-1}$ sec.$^{-1}$*

	Wavelength L (km.)							
	400	600	800	1000	1500	2000	3000	6000
a	1.252	1.318	1.330	1.332	1.333	1.333	1.333	1.333
b	0.358	0.338	0.334	0.333	0.333	0.333	0.333	0.333

TABLE 3.—*The variation of the amplitude with wavelength of the extrapolated solution (46), for the choice $L=400$ km. in order to determine a (=1.252) and b (=0.358) in (49), (50). Here $\Delta x_1=100$ km., and ρ, U, Δt, and β are as in table 2.*

Wavelength L (km.)								
400	600	800	1000	1500	2000	3000	4000	6000
1.000	0.915	0.899	0.895	0.894	0.894	0.894	0.894	0.894

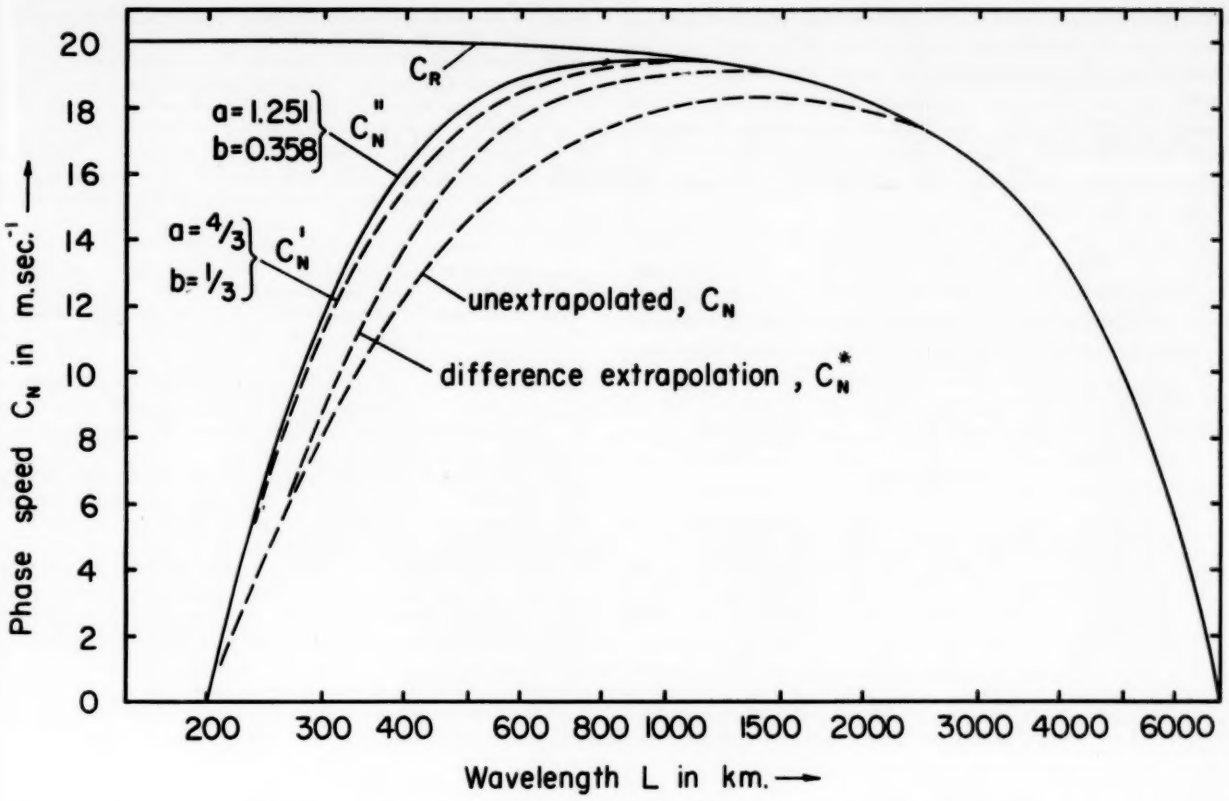

FIGURE 5.—The variation of the numerical phase speed C_N'' of (51) with L for the "optimum" solution extrapolation at $L=400$ km., for the case $\Delta x_1=100$ km. Also shown for comparison are the corresponding phase speeds C_N' (43) for the usual solution extrapolation technique. C_N^* (31) for the difference extrapolation technique, C_N for the unextrapolated solution, and C_R (32), the Rossby (continuous) phase speed. Here $\Delta t=1$ hr., $U=20$ m. sec.$^{-1}$, and $\beta(45°)=1.619\times10^{-13}$ cm.$^{-1}$ sec.$^{-1}$

in the form

$$\varphi_m^{i+1}-\mu\varphi_m^i=(1-\mu)\left(\frac{\varphi_{m+1}^i+\varphi_{m-1}^i}{2}\right), \qquad (53)$$

we may examine this relationship in more detail.

In (53), the superscript i denotes an "unsmoothed" value, and $i+1$ denotes a (once) "smoothed" value, while μ is the "smoothing index". We notice that on a formal basis the larger-mesh solution φ_{m2} corresponds to the local smoothed variable of Shuman, the smaller-mesh solution φ_{m1} corresponds to the local unsmoothed value, and the extrapolated solution φ'_m corresponds to the local space average of the unsmoothed variable of Shuman. With this interpretation the two procedures complement each other, and might well be employed together. For example, one could apply an extrapolation technique and *then* apply a smoothing operation, with the result that the behavior of those wavelengths retained by the smoothing would be better than if smoothing alone were applied. With $\Delta x_1=100$ km., say, and $\rho=2$, this could be accomplished with (40) and a smoothing operator of the Shuman type designed to suppress waves of length ≤ 600 km.

7. CONCLUSIONS

The technique of extrapolating finite-difference estimates to effective zero mesh size systematically reduces the truncation error of solutions of the linear barotropic vorticity difference equation. This technique increases the numerical phase speeds toward the continuous solution's speeds, especially for the shorter waves, while preserving the solution's amplitude. The extrapolation of entire difference solutions found with two different mesh sizes results in an even greater phase speed improvement, and may be adjusted to give optimum results in the vicinity of selected wavelengths. While this "extrapolation of solution" technique improves the solution's phase speed, it introduces an amplitude distortion of certain wavelengths. The ordinary solution extrapolation method introduces about a 10-percent amplitude increase for the shorter waves only, while the "optimum" method introduces about a 10-percent amplitude decrease for *all* of the longer waves, and is consequently unsuitable for routine use. The method of "extrapolation by differentials," formally equivalent to the use of the higher-order difference

584984—61——2

approximations, may then be the best that can be expected from the extrapolation techniques. Whether the increased computation required by even this method is justified by the increased accuracy must await an actual numerical integration. Such a test is particularly important in view of the general observation that higher-order difference schemes often fail to provide the accuracy expected (Richtmyer [7]).

Although the implicit difference scheme has been employed in this analysis for convenience, the techniques described are in no way restricted to it. Noting that the numerical phase speeds of solutions found with the implicit difference scheme are less accurate than those found, say, with the first-forward-then-centered scheme (Gates [2]), an extrapolation technique with the latter difference scheme could be expected to give correspondingly more accurate results.

REFERENCES

1. R. A. Buckingham, *Numerical Methods*, Pitman and Sons, London, 1957, 597 pp. (See pp. 558–559.)
2. W. L. Gates, "On the Truncation Error, Stability, and Convergence of Difference Solutions of the Barotropic Vorticity Equation," *Journal of Meteorology*, vol. 16, No. 5, Oct. 1959, pp. 556–568.
3. C. R. Hartree, *Numerical Analysis*, University Press, Oxford, 1952, 287 pp. (See pp. 139–141.)
4. E. Knighting, "The Reduction of Truncation Errors in Symmetrical Operators," *Technical Memorandum*, No. 3, Joint Numerical Weather Prediction Unit, Washington, D.C., 1955, 5 pp.
5. E. Knighting, D. E. Jones, and M. K. Hinds, "Numerical Experiments in the Integration of the Meteorological Equations of Motion," *Quarterly Journal of the Royal Meteorological Society*, vol. 84, No. 360, Apr. 1958, pp. 91–107.
6. L. F. Richardson, "The Deferred Approach to the Limit," *Philosophical Transactions of the Royal Society of London*, vol. 226 (A), 1927, pp. 299–349.
7. R. D. Richtmyer, *Difference Methods for Initial-Value Problems*, Interscience Publishers, Inc., New York, 1957, 238 pp. (See p. 24.)
8. M. G. Salvadori, "Extrapolation Formulas in Linear Difference Operators," *Proceedings, First U.S. National Congress on Applied Mechanics*, American Society of Mechanical Engineers, New York, 1951, pp. 15–18.
9. F. G. Shuman, "A Method of Designing Finite-Difference Smoothing Operators To Meet Specifications," *Technical Memorandum* No. 7, Joint Numerical Weather Prediction Unit, Washington, D.C., 1955, 14 pp.
10. P. D. Thompson, "Reduction of Truncation Errors in the Computation of Geostrophic Advection and Other Jacobians," *Technical Memorandum* No. 1, Joint Numerical Weather Prediction Unit, Washington, D.C., 1955, 16 pp.

TIME SECTION AND HODOGRAPH ANALYSIS OF CHURCHILL ROCKET AND RADIOSONDE WINDS AND TEMPERATURES

SIDNEY TEWELES

U.S. Weather Bureau, Washington, D.C.

[Manuscript received February 3, 1961

ABSTRACT

Winds and temperatures to above 80 km. measured during the International Geophysical Year by grenade, sphere accelerometer, and Pitot-static tube experiments at Churchill, Manitoba are combined with radiosonde data in time sections. The resulting analyses are discussed in reference to 10-mb. constant pressure charts showing the horizontal circulation near the 30-km. level. Periods in July, August, and December 1957 and January–February 1958 are covered.

The nature of the circulation in successive layers of the stratosphere and mesosphere is suggested by this investigation. In summer, irregular wind flow that is predominantly from the east appears in the middle and upper stratosphere. Strong easterlies in the lower and middle mesosphere are bounded in the upper mesosphere above 75 km. by a sharp vertical wind shear layer with highly variable west winds above, suggesting the existence of rapidly moving, intense cellular circulations near the mesopause. In winter when the boundary of the polar night is close to Churchill, such circulations seem to extend into lower layers until in January they occupy the entire mesosphere.

Strong west winds develop in the mid-stratosphere of wintertime, and a temperature minimum appears near the 30-km. level. During January 1958 the strong westerlies and the temperature minimum as well were disrupted by sudden warming of the entire stratosphere. The vertical structure of this warming effect, as it moved westward across the Atlantic and first appeared at the 40-km. level over Churchill, is shown by means of a cross section.

1. INTRODUCTION

Until recent years there has been a tendency to consider conditions from 20 to 90 km. above the earth either as quiescent or else dominated by zonal motions that change little from day to day but substantially from season to season. There has been great uncertainty about the magnitude of interdiurnal variations at these high levels. Data of the sort presented here help to shed light on this problem.

A remarkable series of temperature and wind observations was made at Churchill, Manitoba during the International Geophysical Year by means of grenades, sphere accelerometers, and Pitot-static tubes carried aloft in rocket vehicles. The grenade experiments are described, data presented, and copious references given by Stroud, Nordberg, and Walsh [15] and Stroud, Nordberg, Bandeen, Bartman, and Titus [13, 14], while accelerometer and static tube experiments are similarly described by Jones, Peterson, Schaefer, and Schulte [5, 6] and Ainsworth, Fox, and LaGow [1], respectively.

In this paper, the results of these experiments are presented in a somewhat different manner to bring out further details of the temperature distribution and circulation of the upper stratosphere and mesosphere. In each of the four cases discussed, radiosonde data are used to determine the analysis up to the 30-km. level during a two- or three-week period centered on the days of the rocket soundings. For higher altitudes, data from rocket experiments are available for two or more observations during each of the four periods. Many facets of the data and their meteorological implications already have been discussed in papers by those responsible for these experiments. Unavoidably, some points are repeated here in developing additional conclusions.

The reliability of conclusions drawn in the following discussion is determined by the accuracy of the data. Stroud et al. [14] state that the errors of the grenade experiment data below 75 km. are generally less than ± 3 C. for temperature, and ± 5 m.sec.$^{-1}$ and ± 15 degrees for wind speed and direction, respectively. Above 75 km. the size of the errors may increase rapidly by a factor of as much as ten at the very highest points. Jones et al. [5, 6] estimate the probable temperature error of the accelerometer experiment to be about 2 percent (4°–6° C.) below 75 km. and 5 percent (10°–15° C.) above 75 km. Furthermore, the dependence of the acceleration upon air density and drag coefficient limits the useful range of the experiment to the layer from 25 km. to 80 km. Temperatures from the static tube experiment are derived from density data having an estimated measurement error of less than 2 percent at 80 km. (Ainsworth et al. [1]).

The wind and temperature values given for the rocketsonde observations are averages for the layer between points at which two grenades exploded; thus, maximum

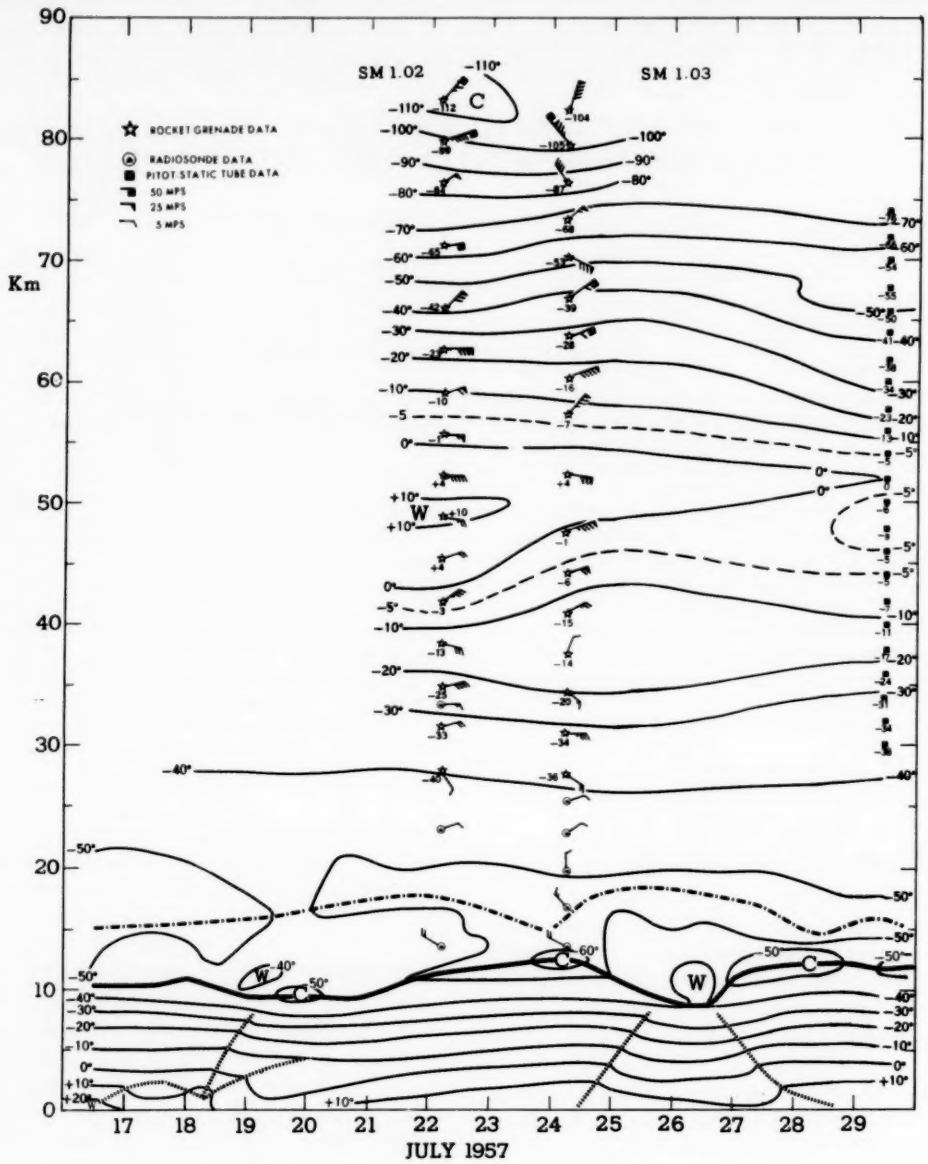

FIGURE 1.—Time section for Churchill, Manitoba, July 17–29, 1957, including data from rocket grenade experiments at 0416 GMT July 22 and 0530 GMT July 24, and a Pitot-static tube experiment at 2200 GMT July 29. Temperature analysis in °C. is based on radiosonde data below 30 km. and on grenade data at higher levels. Grenade temperatures and winds and selected winds from special radiosonde observations are included. Fronts given by dotted lines, tropopause by heavy line, thermal boundary by dash-dot line. C and W indicate cold and warm areas of diagram, respectively. Barbs representing wind speed are placed at the tail end of the wind shafts which point in direction toward which wind is blowing, with north at top of diagram and east at the right.

and minimum values tend to be smoothed out to some extent. Furthermore, random errors will have opposite signs in adjacent layers when the source of error is difficulty in accurate timing of sound arrivals from the grenade at the boundary between the layers. In excessively thin layers, less than 3 km., errors may be greatly magnified. Where highly incompatible values suggested such errors, the effect was minimized by combining adjacent layers.

2. THE CASES OF JULY AND AUGUST 1957

In their broad features, the time sections for July (fig. 1) and August (fig. 2) 1957 are remarkably similar. In the

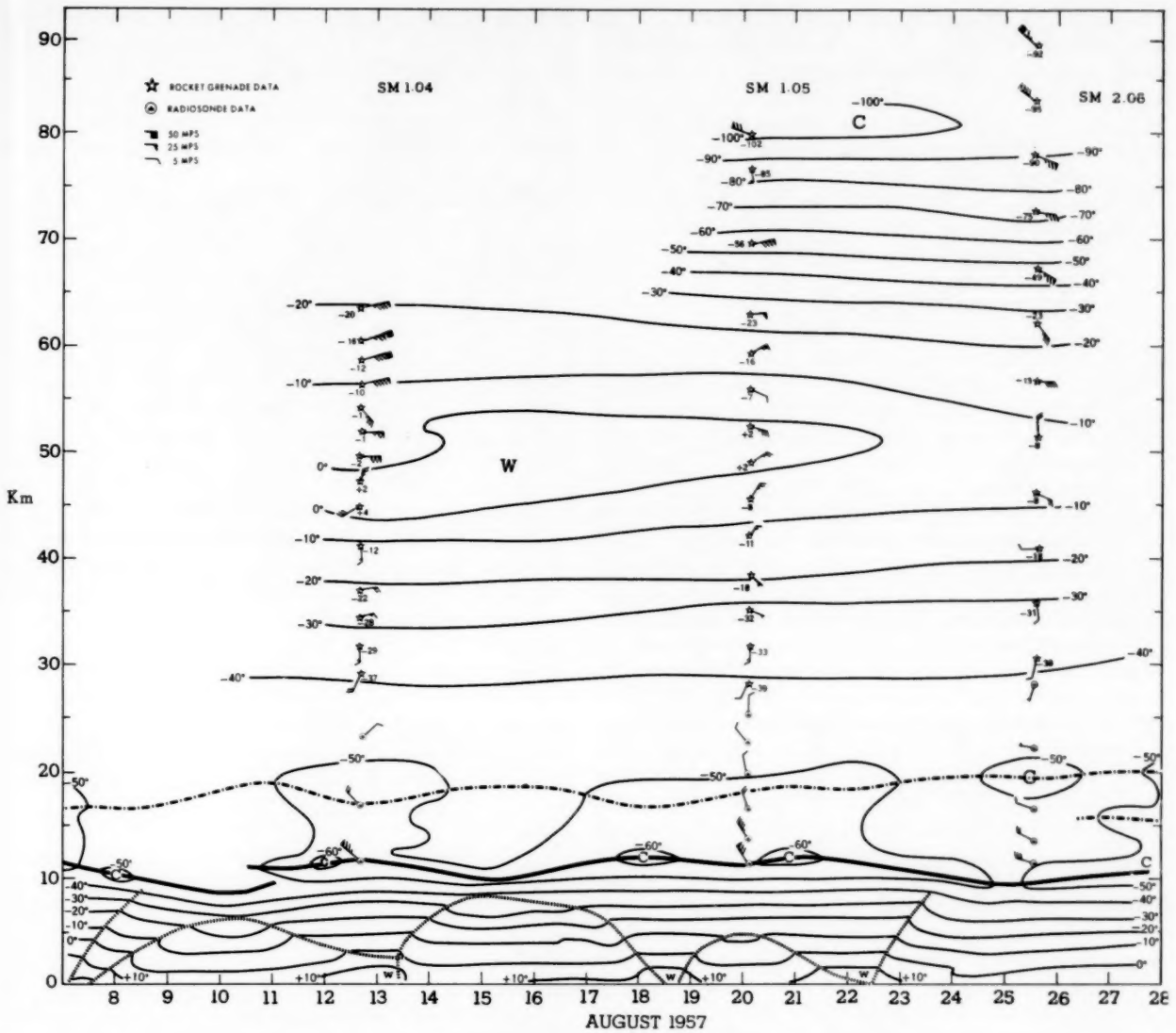

FIGURE 2.—Time section for Churchill, August 8–28, 1957. Rocket grenade experiments are for 1600 GMT August 12, 0230 GMT August 20, and 1408 GMT August 25. Explanation as in figure 1.

lower stratosphere, in each case, there was marked counteraction to tropospheric activity; e.g., warming occurred in this layer simultaneously with the tropospheric cooling following cold front passages. Vertical wind shear, operating in the troposphere to produce a wind maximum at the tropopause, was reversed within this layer so that light winds were found at the top of the layer. There, near 18 km., we find a poorly defined surface of minimum temperature having elevation changes out of phase and temperature changes in phase with those of the tropopause. This boundary seemed to mark the upper limit of tropospheric influence upon stratospheric conditions, for in the 20- to 30-km. layer the winds remained light and temperature constant from day to day. During the July period and continuing into the August period, the temperature varied by only a few degrees, suggesting that there was little vertical motion and almost perfect radiative equilibrium in the layer.

From 18 km. up to the stratopause, the thermal maximum at the top of the stratosphere near 50 km., the temperature increased from about −50° C. to about 0° C. The double temperature maximum at the stratopause on July 29 and again on August 12, already noted by Ainsworth et al. [1], is an interesting phenomenon that might

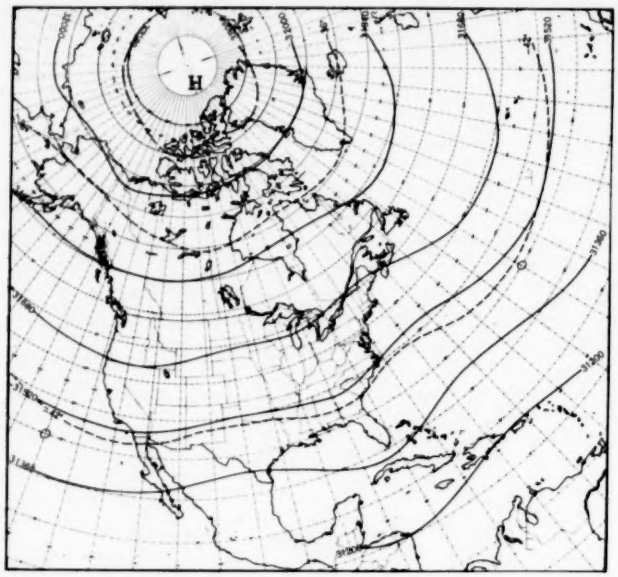

FIGURE 3.—10-mb. chart for 1200 GMT, July 25, 1957 (from [18]). Contours at 160-m. intervals; intermediate contours given by long-dashed lines; isotherms given by dashed lines at 6° C. intervals. H is for high pressure center, L for low pressure center.

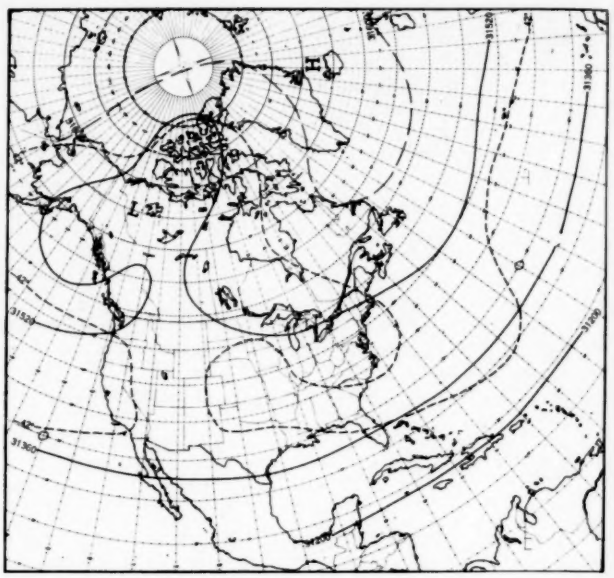

FIGURE 5.—10-mb. chart for 1200 GMT, August 25, 1957 (from [18]). Explantation as in figure 3. Colder air is in the Tropics and near low center in Canada.

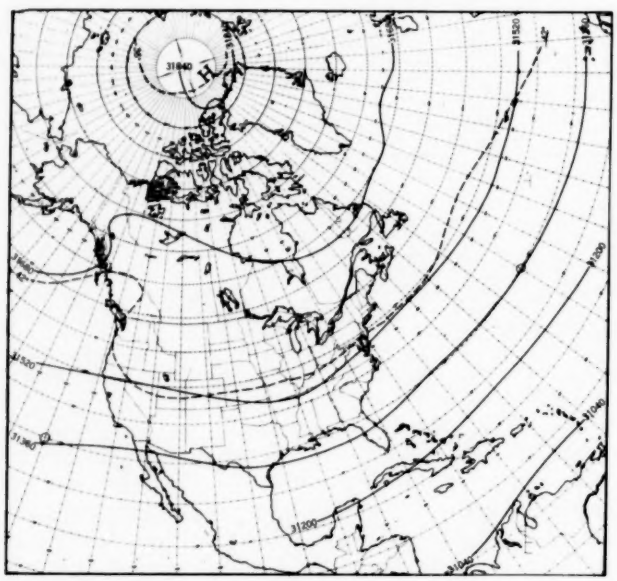

FIGURE 4.—10-mb chart for 1200 GMT, August 15, 1957 (from [18]). Explanation as in figure 3.

be due either to differential heating of layers or to advective processes. In the mesosphere above 50 km., the temperature decreased slightly up to 60 km. but then decreased at an average rate of 4° C. km.$^{-1}$ up to about 80 km. Although on July 24 and again on August 25 a surface of minimum temperature defining the mesopause or top boundary of the mesosphere appeared near 80 km., the rate of temperature rise above that level was very slight.

During July, winds at 10 mb. (30 km.) over North America were everywhere from the east as illustrated by contours of figure 3. On July 22 and 24 at Churchill (fig. 1), the east wind tended to increase with height above 30 km. to speeds exceeding 50 m. sec.$^{-1}$ in the middle and upper mesosphere where the wind backed to northeast or northerly. If the temperature variation between the two observations and the isotherm gradients indicated by the wind shears are taken at face value and interpreted with the aid of the thermal wind equation, the conclusions made in the following paragraphs are valid.

The air in the 40- to 50-km. layer cooled by about 7° C. in the 2-day period. The change of vertical wind shear from easterlies diminishing with height to easterlies increasing with height requires that greater cooling took place to the south of Churchill than to the north.

In the layer from about 45 to 64 km., the observed vertical wind shear of about 2 m. sec.$^{-1}$ km.$^{-1}$ would have required a north-to-south temperature gradient of 7° C. in 10° of latitude, although this rate of horizontal temperature variation would have had to extend beyond the vicinity of Churchill only if vertical wind shear did also. However, since the actual wind was nearly parallel to the thermal wind, the advective wind was negligible and

little horizontal temperature advection or vertical motion along isentropic surfaces is indicated.

At 83 km. on July 22, a remarkably low layer-mean temperature of −112° C. was reported; the decrease of easterly wind speed reported between 80 and 83 km. would have permitted even lower temperatures to the north of Churchill.

By the end of August (fig. 2) temperatures in the troposphere and middle stratosphere were about 5° C. cooler than in July. Cooling was more marked at the stratopause where the temperature was more than 10° C. lower on August 25 than on July 22. The north-to-south temperature gradient that was present in July in the upper stratosphere near Churchill seems to have been destroyed by August 25 when the winds in that layer showed no definite vertical shear. This apparently signals the beginning of that part of the year when temperatures near the level of the stratopause decrease toward the north. Indeed, the 10-mb. charts for August 15 and 25 (figs. 4 and 5) show that such seasonal temperature and wind changes were taking place in the middle stratosphere with gradual formation of a cold Low over northwestern Canada. The 10-mb. temperatures for the remainder of the year at Churchill continued to decrease, particularly rapidly in September and October. Westerly winds appeared at 10 mb. early in September and increased in strength throughout the autumn.

In the mesosphere up to 65 km. during August, a persisting north-to-south temperature gradient is indicated by the increase of the easterly wind component with height. Although the August 12 sounding was cut off near 65 km., it shows easterly winds as strong as those reported in July. However, in the 50–75-km. layer of the mesosphere, the two later August rocket soundings show progressively lighter easterly components and lower temperatures.

Near the mesopause there was a pronounced vertical wind shear with wind shifting from strong easterly to strong westerly, indicating a strong horizontal temperature gradient of about 2° C. per latitude degree toward the north in the 70–80-km. layer on August 20 and 4° C. per latitude degree in the 78–83-km. layer on August 25. The temperature of the mesopause was progressively warmer in each observation from July 22 to August 25. However, the horizontal temperature gradient required by the vertical wind shear across the mesopause on August 25 would have permitted the −112° C. temperature of the July case to be found only 5° latitude to the north of Churchill.

Murgatroyd [9] presented a vertical temperature distribution for summer at 60° N. that is confirmed in most respects by the Churchill summer soundings. Among the principal points of difference are his relatively high temperatures of +21° C. and −93° C. at the stratopause and mesopause respectively. His temperatures for the mesosphere between these levels do not differ greatly from those of the grenade experiments since he gives a greater temperature lapse rate immediately above the stratopause and a lesser lapse rate just below the mesopause than do the grenade experiments. The lapse rates of the grenade experiments thus favor a maximum of vertical mixing in the layers just below the mesopause. The winds observed differ in two respects from those given by Murgatroyd for summer conditions near 60° N. The Churchill data indicate higher wind speeds, exceeding 25 m. sec.$^{-1}$ in the 60- to 75-km. layer, and a shift to west winds near 80 km. elevation instead of near 90 km.

3. THE CASE OF DECEMBER 1957

The time section for December 6–20, 1957 (fig. 6) shows a troposphere 25° C. colder than it was in summer. Above the tropopause, with average height about 1 km. less than in August, the lower stratosphere had cooled only 10° C. The middle stratosphere underwent more remarkable changes, the wind having increased to westerly 25 to 50 m. sec.$^{-1}$ as a 30° C. decrease of temperature at 28 km. produced an inversion base at that altitude. A broad trough with coldest air at the pole dominated Canada at the 30-km. level (fig. 7).

Like the lower stratosphere the stratopause cooled only 10° C. The position of the stratopause at 51 km. is at variance with the position near 60 km. given by Murgatroyd [9] for winter at this latitude. In fact, these experiments show a remarkable temperature minimum near 60 km. The height of the stratopause in January (fig. 8) was indefinite but somewhat closer to 60 km. The extreme temperature changes above 60 km. during the December 12–14 period are in strong contrast to the regularity in temperature patterns of the summer mesosphere. Coupled with winds in the neighborhood of 100 m. sec.$^{-1}$, these temperature changes suggest the existence of violent storms in the winter mesosphere, albeit they are tempests in a near vacuum. Determination of the geographical extent and speed of motion of these storms requires a synoptic network of rocketsonde stations such as that now being activated over North America.

The wintertime temperatures of the upper mesosphere at Churchill were much warmer than those measured there in summer or at lower latitudes in winter. Although warming in the stratosphere and mesosphere is generally explainable by a reasonable amount of sinking and compression of air from higher layers, Kellogg [7] has described a process by which heat may be liberated at or above the mesopause through recombination of atomic oxygen brought down from ionospheric layers rich in this element.

4. THE CASE OF JANUARY–FEBRUARY 1958

Even before the rocketsonde data became generally available, the radical changes in stratospheric circulation and accompanying explosive warming of the stratosphere during the weeks following mid-January 1958 had been the subject of several papers (Boville [3]; Palmer [10];

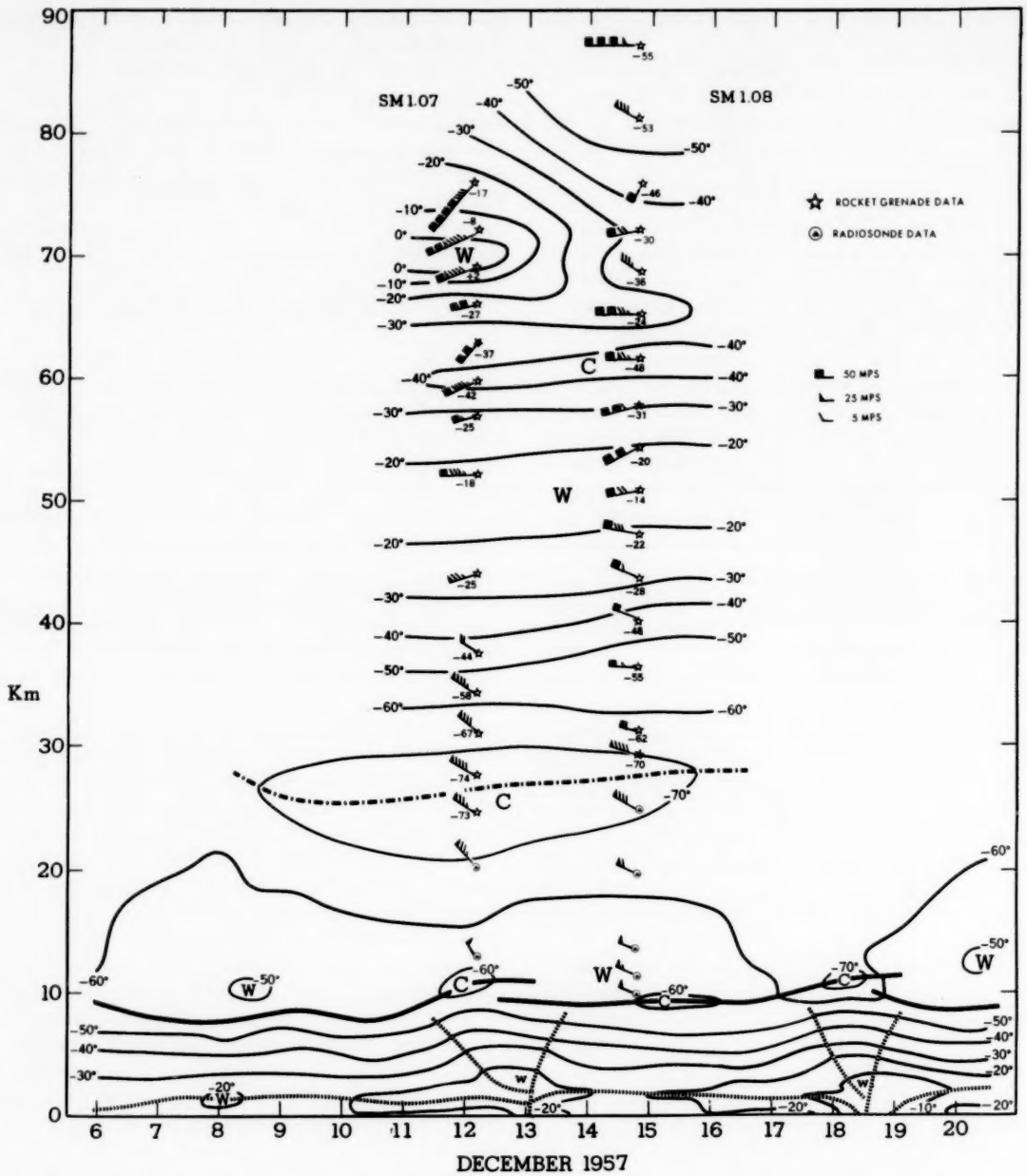

FIGURE 6.—Time section for Churchill, December 6–20, 1957. Rocket grenade experiments were at 0400 GMT December 12 and 2100 GMT December 14. Explanation as in figure 1.

Scherhag [11, 12]; Teweles and Finger [16]; Teweles, Rothenberg, and Finger [17]).

Because most frontal activity in the troposphere was displaced far to the south of Churchill during the period January 22 to February 6, only relatively minor changes in tropopause height and temperature are revealed in figure 8. In the lower stratosphere, unusual warming after January 26 culminated in a temperature of −41° C. at 100 mb. on February 3. In mid-stratosphere by January 25, the 30-km. temperature had dropped below −70° C., and by January 27 the altitude of the temperature minimum was raised to 33 km. This temperature minimum was depressed to 25 km. in the succeeding days as strong warming occurred in the upper stratosphere.

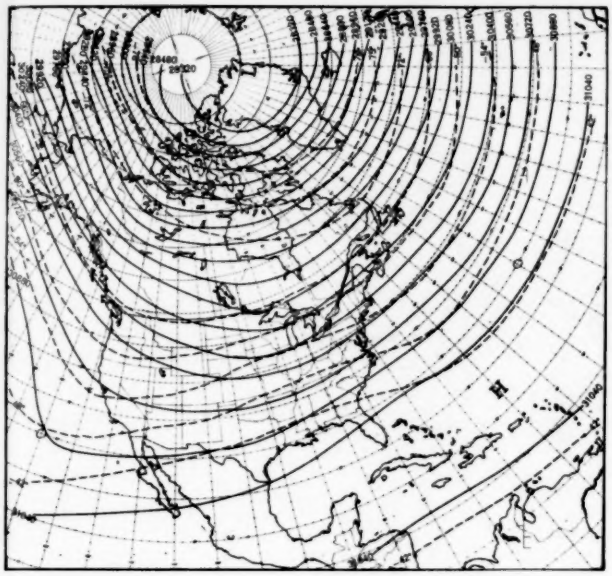

FIGURE 7.—10-mb chart for 1200 GMT, December 15, 1957 (from [18]). Explanation as in figure 3.

For the period January 25 to 29, an unprecedented concentration of rocket sounding data is available for reconstructing conditions at high levels. Accelerometer spheres launched by Nike-Cajun rockets on January 25 and 29 gave both up-leg and down-leg information. Down-leg information was given by a similar sphere, borne by one of two grenade-carrying Aerobee rockets launched on January 27. The temperatures derived from these accelerometer experiments become consistent with radiosonde data at and above the 25-km. level, and above the ceiling of the radiosonde data remain consistent internally and with grenade data up to 65 km.

Warming took place slowly at Churchill between 40 and 45 km. from January 25 to 27, then rapidly between 30 and 60 km. from January 27 to 29. The 4-day temperature increase of almost 70° C. in the 38- to 41-km. layer at Churchill is greater than any ever recorded at lower levels.

The circulation and thermal structure at levels above 30 km. on January 27 can be reconstructed by hodograph analysis (fig. 9) of grenade experiment winds for that day (shown on fig. 8). From the tropopause up to 65 km., there is remarkable agreement in the winds from these two experiments. A southwest wind of 30 m. sec.$^{-1}$ was observed just below the tropopause at 8 km. as a trough approached from the west. The wind decreased upward to a minimum near 14 km. and increased again to a maximum of about 75 m. sec.$^{-1}$ from the north-northeast at 33 km. The resulting shear vector in the 8- to 33-km. layer placed the warmest air toward the northwest. Thus there was a cold Low to the east and a warm High to the west of Churchill with maximum intensity at 33 km. There have been few cases in which the level of a polar night jet stream of such strength has been so clearly defined. Above the 33-km. level, the decrease in strength of the jet required a reversal of temperature gradient. Thus the Low became a warm Low and the High became a cold High, both systems decreasing in strength with elevation. These features characterize the 33-km. level as a null level, as described by Faust and Attmannspacher [4] (or see Lamb [8]).

Near the 45-km. level the wind shifted around through easterly to become strong southerly at 52 km. Apparently the vertical axis of low pressure sloped from east to west across the Churchill area at about the 45-km. level, with the low center itself south of Churchill at that level. The south wind increasing with height in the 45- to 52-km. layer required a warm High to the east and a cold Low to the west, both systems increasing in strength with elevation to at least 52 km. The advective wind in the 33- to 52-km. layer can account for a warming of about 30° C. in two days. Since a warming of 60° C. was actually observed at 40 km. during the two days ending on January 29, and since the final temperatures are undoubtedly anomalously high for that level, subsidence as well as advection must be called upon to explain such a great warming.

Above 52 km. the circulation apparently retained its general form and strength to at least 75 km. Although the reported winds were very erratic, mean winds for overlapping 10-km. layers up to 75 km. were quite consistently from the south.

As in the December case, the alternation of warm and cold air layers was in sharp contrast to the steep lapse rate of the summer mesosphere, and the temperature in the upper portion of the mesosphere was much warmer than in summer.

In the 0604 GMT sounding, a remarkably strong west wind was reported along with high temperature at 79 km. By 1845 GMT, west winds were reported at all levels above 77 km. Expansion of the warm layer near 80 km. during the next two days is indicated by the falling-sphere data. Here we see the approach to Churchill of a system similar to that which moved away from Churchill between December 12 and 14. The reality of the large variations that are reported in wind speed and direction from one level to the next or between observations only a few hours apart must be more firmly established before great confidence can be placed in the features of the circulation inferred from the observations. Even so, it is now certain that the wintertime circulation of the mesosphere, in the subarctic, is very active and thus of very special interest to the meteorologist.

5. EVENTS IN SURROUNDING AREAS AT TIME OF WARMING AT CHURCHILL

The 1200 GMT 10-mb. charts for January 25 (fig. 10), U.S.

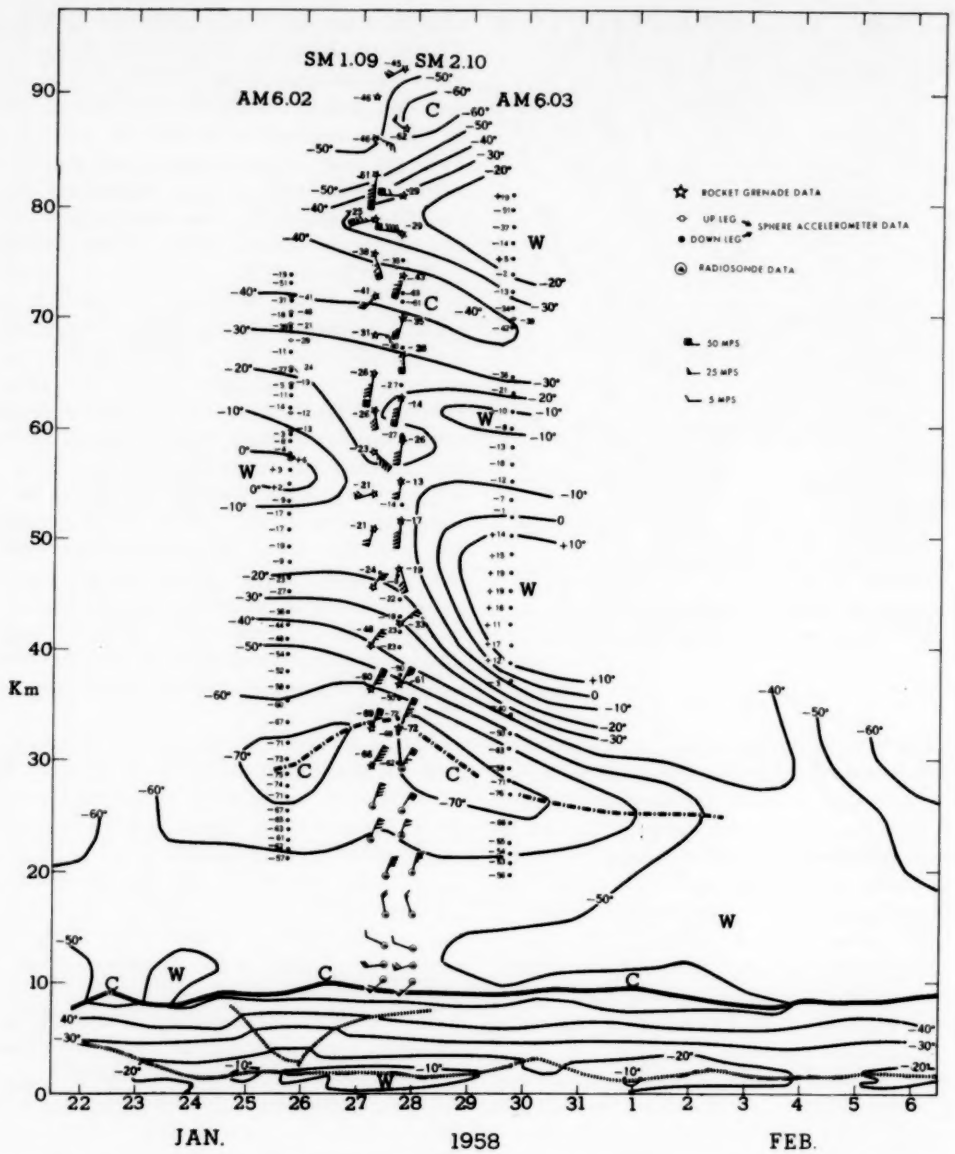

FIGURE 8.—Time-section for Churchill, January 22–February 6, 1958. Rocket grenade experiments were at 0604 GMT and 1845 GMT January 27. Sphere accelerometer experiments were at 1912 GMT January 25, 1845 GMT January 27, and 1906 GMT January 29. Explanation as in figure 1.

Weather Bureau [18], and for January 29 (fig. 11), Behr et al. [2], help to place the Churchill rocket sounding data near the 30-km. level in perspective with events that were taking place in surrounding portions of the hemisphere. These charts confirm the existence of the relatively cold Low revealed by the wind and its vertical variation near this level on January 27. In the 4-day interval, this Low rapidly approached Churchill from a position over southern Greenland. Meanwhile, the warm High in the Gulf of Alaska moved poleward across Alaska into the Arctic Ocean.

During early January, a section of the polar night jet stream, which was nearly circumpolar in December (fig. 7), slowly arched poleward across Alaska. By January 25, the axis of this current stretched across the North Pole southward toward Churchill, and the Arctic was being ventilated with warm air from sunlit latitudes. The exceedingly cold air that formerly occupied the Arctic

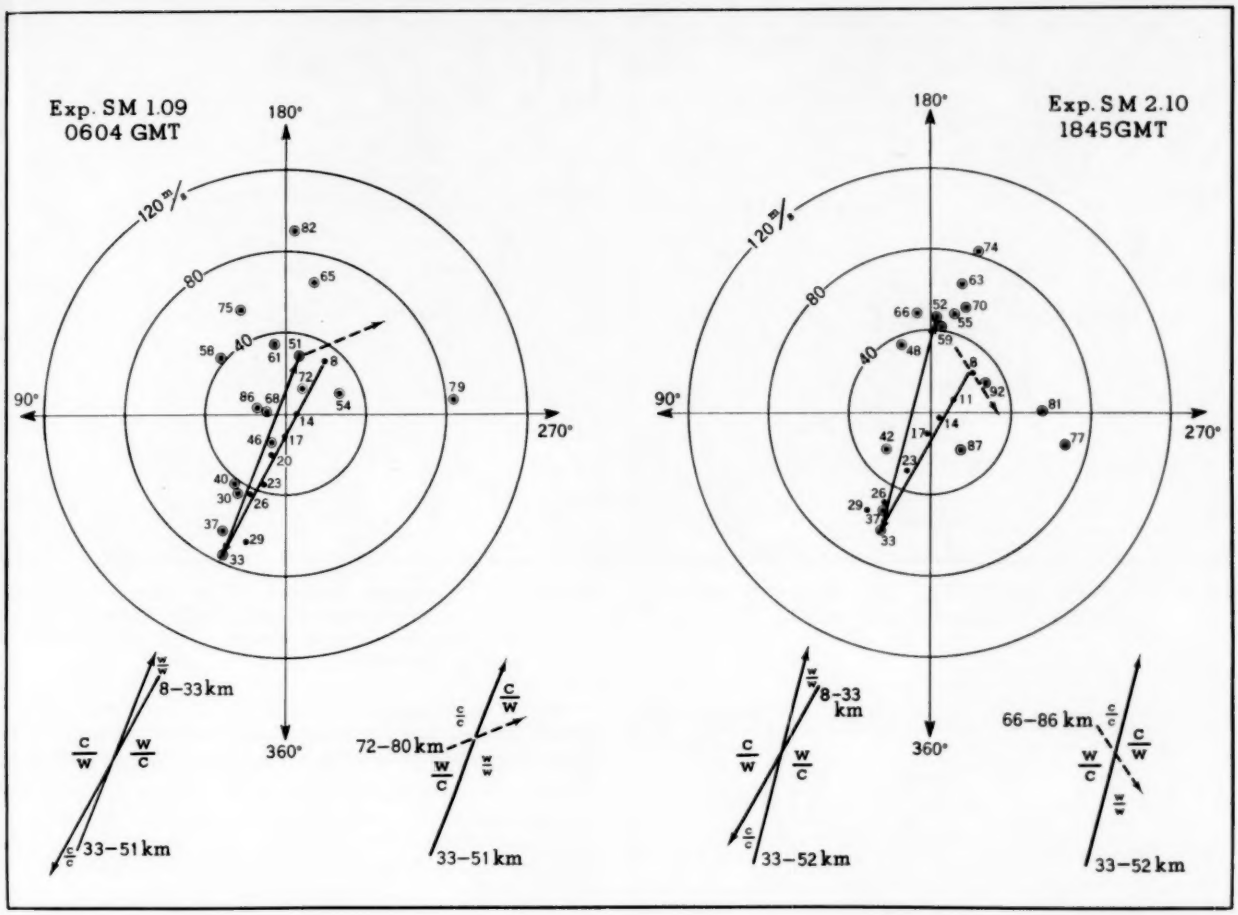

FIGURE 9.—Hodographs of the wind observations plotted in figure 8. Radiosonde winds given by dots to represent head of arrow with tail at origin; arrow points in direction wind is blowing. Circled dots represent grenade experiment winds, numbers at dots give height of mid-point of layer to the nearest km. Arrows in diagram give vertical wind shear in layers having relatively uniform shear. Two or three points were averaged where indications were indefinite. Shear arrows for layers are superimposed below hodograph. Relatively warm direction in the shear layer is indicated by W, cold direction by C; thus, W/C indicates the direction of greatest static stability with relatively warm layer lying above relatively cold layer. Near 60 km. there is a neutral layer without significant shear lying between layers with shear. Shear of the highest layers, given by dashed arrow, is somewhat indeterminate.

split into two cells, one associated with low pressure over Siberia (see Behr et al. [2]), the other centered in the western portion of the low pressure area approaching Churchill from the east.

Hodograph analysis for January 27 (fig. 9) when applied to the 10-mb. circulation pattern leads to several interesting conclusions. The polar night jet stream at Churchill had its maximum strength at 33 km. above which it lost strength. Further interpretation is suggested by the pattern of contours and isotherms found at 10 mb. on January 25. The axis of the 10-mb. Low center, located just southeast of Hudson Bay on January 25, from hydrostatic considerations must have sloped with elevation in the direction of coldest air. If the axis of coldest air also sloped in the same direction and the contour-isotherm relationship did not change with height, the vertical wind structure at Churchill can be explained quite convincingly. At 33, km. where the wind shear direction reversed, the cold air was centered directly over Churchill, but the low pressure center was still to the east. Above 33 km., the cold air was centered west of Churchill to at least 51 km., but northerly winds show that the low center remained to the east and southeast up to 45 km. At this level the Low in its westward movement passed south of Churchill between observations. The uniformly strong wind shear between 37 and 52 km. showed the presence of a tight temperature gradient with warmest air toward the east, like that in the southeast quadrant of the Low at 10 mb. (figs. 10 and 11).

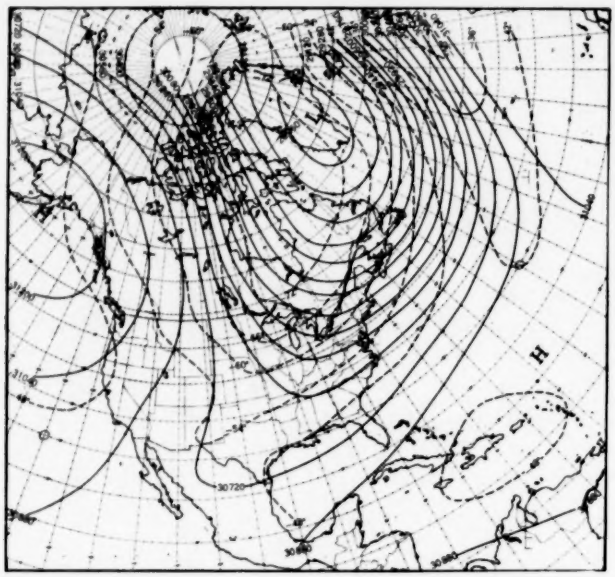

FIGURE 10.—10-mb. chart for 1200 GMT, January 25, 1958 (from [18]). Explanation as in figure 3.

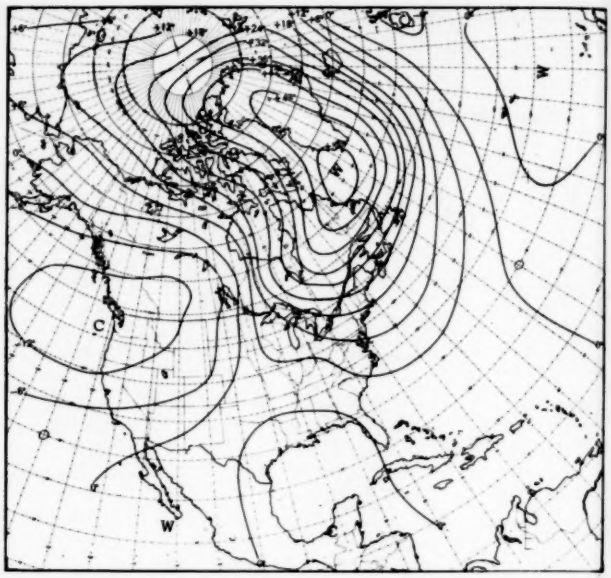

FIGURE 12.—Temperature change in °C. at 10mb. in the 4-day period January 25–29, 1958, obtained by graphical subtraction of isotherm patterns in figures 10 and 11. W indicates area of warming, C area of cooling.

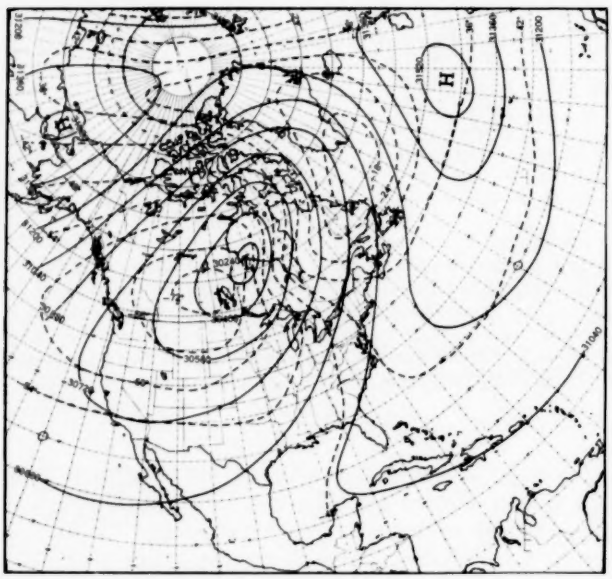

FIGURE 11.—10-mb. chart for 1200 GMT, January 29, 1958 (data from [2]). Explanation as in figure 3.

The 4-day temperature change at 10 mb., computed from the isotherm patterns of January 25 and 29 (fig. 12), shows a remarkable rise of more than 54° C. in the region between Greenland and Labrador. The even larger temperature change at the 40-km. level above Churchill during the same period was most certainly connected with the warming farther east at 10 mb. This gives convincing proof of the tremendous lateral shift with altitude of stratospheric patterns. In this case, the leading edge of the warming sloped upward 10 km. in a horizontal distance of 2,000 km., the same 1:200 slope typical of warm front surfaces in the lower troposphere.

If the wind reversal near 45 km. is taken as evidence that the low-center position was very close to Churchill at that level, and if the low-center position at 30 km. is taken from the January 27 10-mb. charts of Behr et al. [2], then the axis of the low center tilted westward 1,500 km. in a vertical layer 15 km. deep, a slope of 1:100. The 1:200 slope of the warm air indicates that it was overspreading the top of the low center to diminish the intensity of the center first near 40 km. and gradually at lower levels. The net effect is demonstrated by the great loss of kinetic energy at 30 km. over North America during the following week and over the remainder of the hemisphere by mid-February (see 10-mb. charts in Behr et al. [2] or U.S. Weather Bureau [18]). Simultaneously, the general level of the 10-mb. surface in the Arctic was substantially raised.

A cross-section from Naknek, Alaska through Churchill to Berlin, Germany on January 29 (fig. 13) illustrates the great horizontal and vertical extent of the warming at the time of the 40-km. warming at Churchill. Cooling with the advance of the cold sliver near 30 km. in the lower forward portion of the system is almost as impressive as the warming in the upper rear portion. While the cooling did not produce temperatures that were anomalous for the entire hemisphere as did the concomitant warming, it did

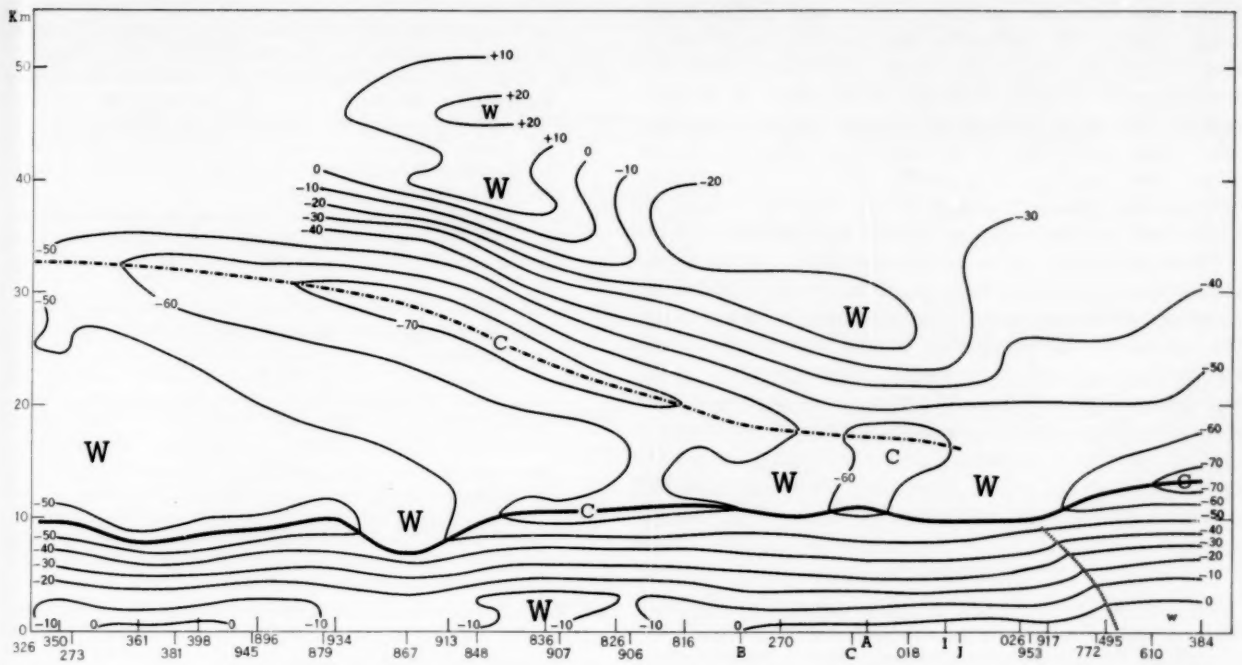

FIGURE 13.—Cross section, January 29, 1958, near 55° N. from Naknek, Alaska (station 326) through Churchill (station 913) to Berlin Germany (station 384). Explanation generally as in figure 1. Temperature analysis at high levels in vicinity of Churchill is based entirely on sphere accelerometer experiment AM 6.03 for 1906 GMT. Identification numbers of radiosonde stations from which data were used are shown along bottom of chart at projected location of station.

bring anomalously low temperatures into the middle latitudes. All indications are that the stratospheric features in the cross-section were slowly moving toward the west. Thus, the warmest air at 25 km. crossed over Berlin on January 25, passed to the south of Greenland on January 29, as shown in figure 12, and then diffused across North America in the first three days of February.

Figure 8 shows the upwelling of the coldest air to above 30 km. that immediately preceded the intensive warming near the 40-km. level. The core of the polar night jet stream seems to have been wedged between these layers of climactic cooling below and incipient warming above.

The interaction of vertical motions and jet stream accelerations around the vertically tilting core of low pressure must account for the observed temperature and pressure changes. Two-dimensional sections do not reveal the exact linkage by which these motions are maintained for long periods in a tremendous volume of atmosphere. However, increasingly detailed descriptions of these phenomena may eventually lead to a successful mathematical formulation of the problem.

6. CONCLUSION

The temperature and wind observations utilized in this paper were among the first to become available to great heights at such high latitudes. The large amount of information deduced from this limited number of soundings is a strong recommendation for gathering much more temperature and wind information to the highest possible levels.

That there are several layers of the atmosphere having their own characteristic types of horizontal circulation is brought out by the charts displayed in this paper. Undoubtedly, the dominating cause is the division of the atmosphere into layers of radically different static stability by the variable effectiveness of its constituents in absorbing radiation at different altitudes, latitudes, and seasons. However, the circulation at any level is tied hydrostatically to the circulation at adjacent levels by the temperature distribution in the intervening layers. Feedback of energy from one level to another may be great or small depending upon the static stability, baroclinicity, and relative pressure and kinetic energy difference between the levels; thus accurate measurement of these parameters is important for future research studies.

High static stability is the only significant unique quality of the stratosphere available to explain the relatively slow development and large size of stratospheric systems compared to those of the troposphere. In developing, these systems carry the seeds of their own destruction, for baroclinicity is dispersed and destroyed as the cold pool is transported from the darkness of the

Arctic into the sunlit latitudes while warm air floods the polar regions. Thereafter the long slow process of formation of a new cold pool in the Arctic must begin again and continue until interrupted by the development of another perturbation or by radiational heating from the returning sun. The upper limit of the layer in which this process takes place has been the subject of much speculation. Strategically planned rocket firings near the poles in winter will certainly help to answer this problem.

Much about the nature of the circulation in the upper stratosphere and lower mesosphere has been revealed by these and other rocket soundings. However, if anything, the nature of the circulation in the upper mesosphere has become more of a mystery. Even though diurnal and semi-diurnal effects and errors in measurement are large near the mesopause, the data presented here indicate that the circulation of nearby layers is really quite active, particularly so in winter through a deep layer at the boundary of the polar darkness.

REFERENCES

1. J. E. Ainsworth, D. F. Fox, and H. E. LaGow, "Measurement of Upper Atmosphere Structure by Means of the Pitot-Static Tube," National Aeronautics and Space Administration, *Technical Note D-670*, 1961.
2. K. Behr, R. Scherhag, and G. Warnecke, "Tägliche Hohenkarten der 10 mbar. Fläche für das International Geophysicalische Jahr 1958, Teil I, 1. Vierteljahr," *Meteorologische Abhandlungen*, Band XIII, Heft 1, Berlin, Freie Universität, 1960.
3. B. W. Boville, "The Aleutian Stratospheric Anticyclone," *Journal of Meteorology*, vol. 17, No. 3, June 1960, pp. 329–336.
4. H. Faust and W. Attmannspacher, "Cell Structure of the Atmosphere," *Final Report*, Zentralamt des Deutschen Wetterdienstes, Offenbach am Main, Germany, Oct. 1959.
5. L. M. Jones, J. W. Peterson, E. J. Schaefer, and H. F. Schulte, "Upper-Air Densities and Temperatures from Eight IGY Rocket Flights by the Falling-Sphere Method," *IGY Rocket Report Series*, No. 5, IGY World Data Center A, Rockets and Satellites, Washington, D.C., Dec. 1, 1959.
6. L. M. Jones, J. W. Peterson, E. J. Schaefer, and H. F. Schulte, "Upper-Air Density and Temperature: Some Variations and an Abrupt Warning in the Mesosphere," *Journal of Geophysical Research*, vol. 64, No. 12, Dec. 1959, pp. 2331–2340.
7. W. W. Kellogg, "Warming of the Polar Mesosphere and Lower Ionosphere in Winter," Abstract in *Bulletin of the American Meteorological Society*, vol. 40, No. 12, Dec. 1959, p. 645.
8. H. H. Lamb, "Some Interesting Properties of the 'Nullschicht' or Maximum-Wind Layer," *Meteorological Magazine*, vol. 86, No. 1019, May 1957, pp. 142–145.
9. R. J. Murgatroyd, "Winds and Temperatures between 20 km. and 100 km.—A Review," *Quarterly Journal of the Royal Meteorological Society*, vol. 83, No. 358, Oct. 1957, pp. 417–458.
10. C. E. Palmer, "The Stratospheric Polar Vortex in Winter," *Journal of Geophysical Research*, vol. 64, No. 7, July 1959, pp. 749–764.
11. R. Scherhag, "Der 'Berliner Phänomen' und das Geophysikalische Jahr," *Wetterkarte des Deutschen Wetterdienstes*, Beilage Nr. 136–137, Berlin, May 1958.
12. R. Scherhag, "Stratospheric Temperature Changes and Associated Changes in Pressure Distribution," *Journal of Meteorology*, vol. 17, No. 6, Dec. 1960, pp. 575–582.
13. W. G. Stroud, W. Nordberg, W. R. Bandeen, F. L. Bartman, and P. Titus, "Rocket-Grenade Observations of Atmospheric Heating in the Arctic," *Journal of Geophysical Research*, vol. 64, No. 9, Sept. 1959, pp. 1342–1343.
14. W. G. Stroud, W. Nordberg, W. R. Bandeen, F. L. Bartman, and P. Titus, "Rocket-Grenade Measurements of Temperatures and Winds in the Mesosphere over Churchill, Canada," *Journal of Geophysical Research*, vol. 65, No. 8, Aug. 1960, pp. 2307–2323.
15. W. G. Stroud, W. Nordberg, and J. R. Walsh, "Atmospheric Temperatures and Winds between 30 and 80 km.," *Journal of Geophysical Research*, vol. 61, No. 1, Mar. 1956, pp. 45–56.
16. S. Teweles and F. G. Finger, "An Abrupt Change in Stratospheric Circulation Beginning in Mid-January 1958," *Monthly Weather Review*, vol. 86, No. 1, Jan. 1958, pp. 23–28.
17. S. Teweles, L. Rothenberg, and F. G. Finger, "The Circulation at the 10-Millibar Constant Pressure Surface Over North America and Adjacent Ocean Areas, July 1957 Through June 1958," *Monthly Weather Review*, vol. 88, No. 4, Apr. 1960, pp. 137–150.
18. U.S. Weather Bureau, *10-Millibar Synoptic Weather Maps, Three Times Monthly, July 1957 Through June 1958 of the IGY Period*, Washington, D.C., Dec. 1959.

THE WEATHER AND CIRCULATION OF JANUARY 1961*

RAYMOND A. GREEN

Extended Forecast Section, U.S. Weather Bureau, Washington, D.C.

1. INTRODUCTION

In the eastern half of the United States the first half of January 1961 was relatively mild under high index circulation, continuing a warming trend which had started late in December [1]. During the second half of January, on the other hand, extremely cold weather prevailed in strong northerly flow between an intense trough along the east coast and a blocking High over western Canada; the cold spell lasted well into February. The highlight of the change in regime was a severe storm on January 19 and 20, 1961, which caused heavy snow in major cities along the east coast from Washington, D.C. to Boston, Mass. Severe blizzard conditions were reported in southern New England where northeasterly gales caused extensive flooding of coastal lowlands.

At no time during the month was the circulation favorable for extensive precipitation over most of the interior of the contiguous United States. This was the driest January in 90 years or more at several stations listed in table 1.

2. TRANSITION WITHIN THE MONTH

Many features of the interesting evolution of the mean circulation can be seen in the charts of 5-day mean 700-mb. height and weekly surface temperature anomalies, figures 1 through 4. During the first week the mean circulation (January 3–7, fig. 1A) consisted of a deep trough from Alaska southward, a rather strong ridge over the northwestern States, and a trough along the east coast of North America from Labrador to Florida. A blocking ridge in the Greenland area, with largest height anomaly in Davis Strait, was joined to the subtropical Atlantic ridge, and a strong cyclonic center was located over the North Sea. The zonal index (not shown) was diminishing slowly from the early January peak which terminated the index cycle of December [1]. However the warming trend noted at the end of December over the contiguous United States continued, and temperatures over half or more of the country averaged above normal (fig. 1B).

By the middle of the second week (January 10–14, fig. 2A), the low center south of Alaska had intensified, while a blocking surge (best seen in the height anomaly pattern) had moved southwestward from Davis Strait to the Great Lakes. A weak trough over the Central Plains moved slowly eastward, and the trough in the western Atlantic grew stronger in the north. While zonal index values continued to diminish slowly, they remained above normal.

This was the warmest week of the month over most of the Nation (fig. 2B). Temperatures averaged above normal over almost the entire country, averaging 10° to 25° above in the north central interior.

One major storm during the week was responsible for moderate to heavy snow from West Virginia to southern New England. Part of this storm intensified off the middle Atlantic coast, causing hurricane-force winds and high seas off the New England coast.

Rapid amplification occurred from the central Pacific to eastern North America during the third week. Midway through the week, the Pacific cyclone reached its greatest intensity (over 1000 ft. below normal, fig. 3A). In the ridge downstream, heights averaged some 800 feet above normal in western Canada. With the Atlantic coastal trough also strong, the flow over central and eastern Canada was meridional, and cold air flowed into the eastern United States.

These conditions accompanied the severe storm of the 19th, which deepened more than 1 mb. per hour for 24 hours over the relatively warm water along the Atlantic coast. This development in turn sustained and intensified the meridional flow, so that the warm temperature regime of previous weeks was effectively ended in the East. New record low temperatures for January 21 and 22 were established in the wake of the storm at New

TABLE 1.—*Stations reporting long-standing records for least January precipitation broken in 1961*

Station	Date records began
Grand Junction, Colo.	1892
Detroit, Mich.	1871
Escanaba, Mich.	1871
Duluth, Minn.	1871
Rochester, Minn.	1886
Kansas City, Mo.*	1888
Akron, Ohio	1887
Sandusky, Ohio	1877
Toledo, Ohio	1870
Chattanooga, Tenn.	1879

*Equaled record.

*Articles describing the weather of February, March, and April 1961 will appear in the May, June, and July 1961 issues, respectively.

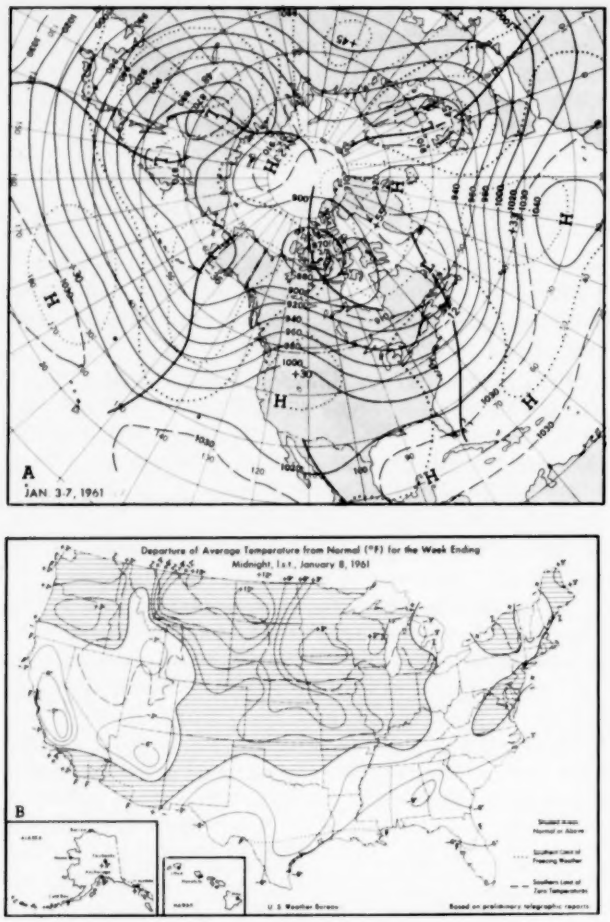
A
JAN. 3-7, 1961
Departure of Average Temperature from Normal (°F) for the Week Ending
Midnight, E.S.T., January 8, 1961
B
U. S. Weather Bureau
Based on preliminary telegraphic reports

FIGURE 1—(A) 5-day mean 700-mb. heights (solid) and departures from normal (dotted), both in tens of feet, for January 3–7, 1961. This represents the mean circulation during the first week of January. Note the positive anomaly center over Davis Strait, indicating the presence of blocking. (B) Departure of average temperature from normal (°F.) for the week ending January 8. Continuation of warming from the previous week was the general rule, except in the South (from [6]).

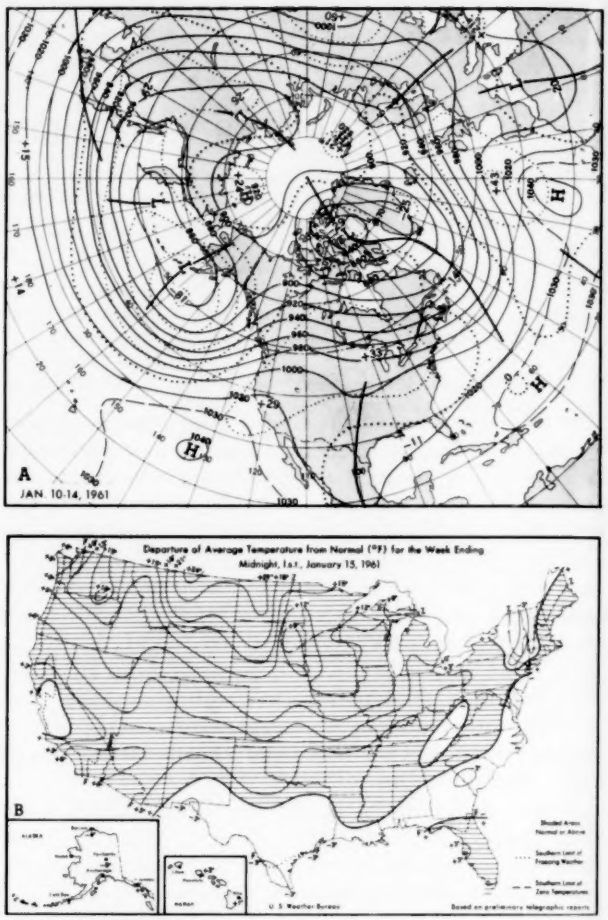
A
JAN. 10-14, 1961
Departure of Average Temperature from Normal (°F) for the Week Ending
Midnight, E.S.T., January 15, 1961
B
U. S. Weather Bureau
Based on preliminary telegraphic reports

FIGURE 2.—(A) 5-day mean 700-mb. heights (solid) and departures from normal (dotted), both in tens of feet, for January 10–14, 1961. By this time a positive anomaly center had retrograded from Davis Strait to the Great Lakes region, and the negative anomaly center south of Alaska had intensified from the previous week. (B) Departure from normal of average temperature (°F.) for the week ending January 15, 1961. This was the warmest week in January (from [6]).

Haven, Conn., Wilmington, Del., Philadelphia, Pa., and for the 22d at Hartford, Conn., Chattanooga, Tenn. and Daytona Beach, Fla. Snowfall ranged from 2 to 16 inches in Maryland, 10 to 30 inches in New Jersey, and 10 to 20 inches over southern New England.

Intense cold dominated the weather east of the Continental Divide during the final week. The long-wave pattern over North America (fig. 4A) remained strongly amplified, and northerly winds continued to transport frigid air into the United States. Sub-zero minima were reported southward as far as Denver, Colo., St. Louis, Mo., Nashville, Tenn., and Richmond, Va. In the South, only Brownsville, Tex., and southern Florida escaped freezing temperatures. Most of the snow cover over the Northeast remained from the previous week, and additional snow accumulated during a final storm which intensified off the Atlantic coast on the 27th.

Comparison of half-month mean charts at 700 mb. in figure 5 reveals the remarkable change in circulation which occurred from the central Pacific to the east coast of North America during the month. Contrast between the relatively zonal pattern of the first half (part A), and the strongly amplified pattern of the second half (part B) was greatest in the Yukon. Positive height changes there (part C) were as much as 800 feet, while changes in the opposite sense were about half this magnitude in the troughs south of the Aleutians and over the Great Lakes. Changes of 700-mb. height anomaly were in the direction

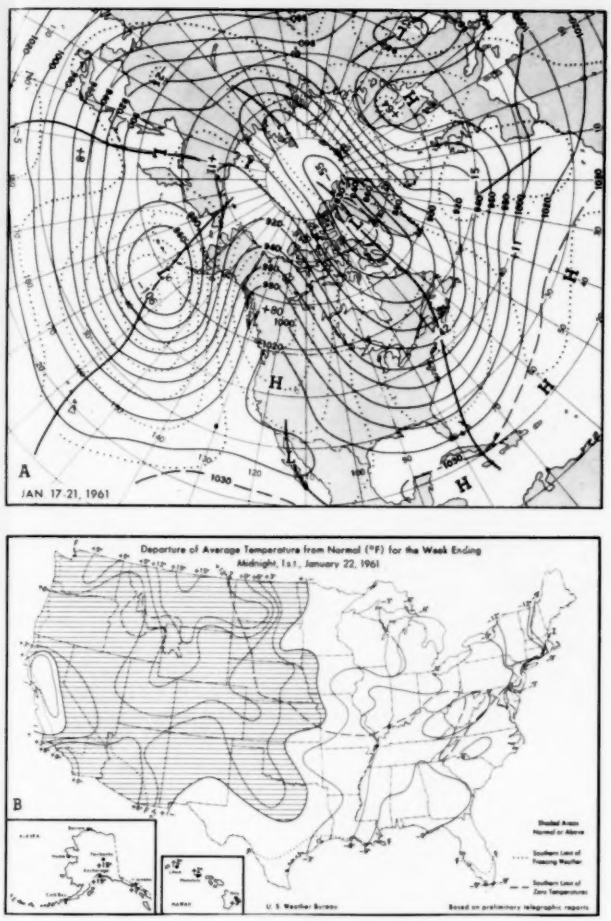
A
JAN. 17-21, 1961
B
Departure of Average Temperature from Normal (°F) for the Week Ending
Midnight, l.s.t., January 22, 1961
U. S. Weather Bureau
Based on preliminary telegraphic reports

FIGURE 3.—(A) 5-day mean 700-mb. heights (solid) and departures from normal (dotted), both in tens of feet, for January 17–21, 1961. By this time the mean wave was strongly amplified from the eastern Pacific to the western Atlantic. An intense storm developed off the middle Atlantic coast this week and temperatures tumbled in the East as shown in (B) Departure from normal of average temperature (°F.) for the week ending January 22, 1961. Most of the cooling occurred after mid-week (from [6]).

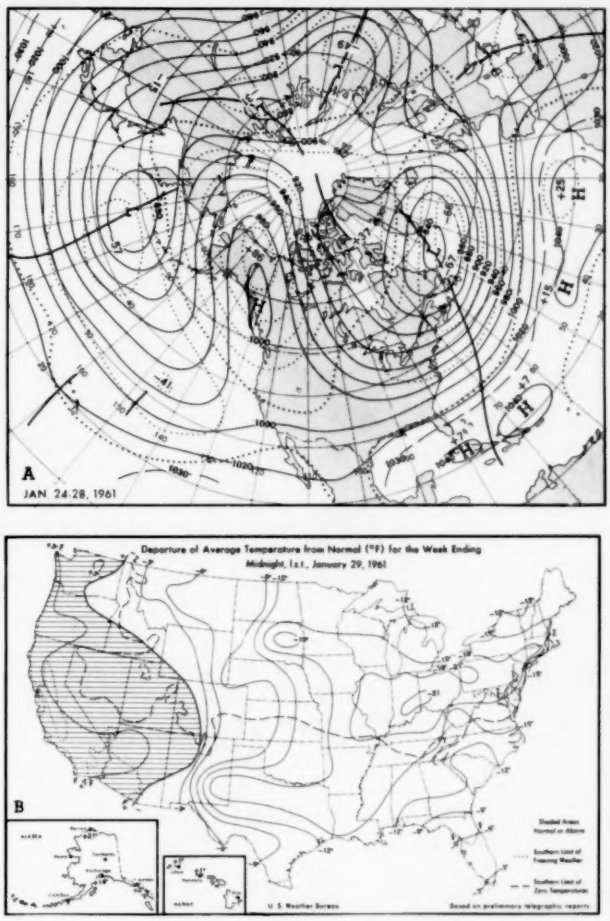
A
JAN. 24-28, 1961
B
Departure of Average Temperature from Normal (°F) for the Week Ending
Midnight, l.s.t., January 29, 1961
U. S. Weather Bureau
Based on preliminary telegraphic reports

FIGURE 4.—(A) 5-day mean 700-mb. heights (solid) and departures from normal (dotted), both in tens of feet, for January 24–28, 1961. Large amplitude of the circulation continued from the previous week over North America. Cold air flooded the United States eastward from the Continental Divide. (B) Departure from normal of average temperature (°F.) for the week ending January 29, 1961. This was the coldest week of the month (from [6]).

favoring lower temperatures east of the Rockies. The close relationship of positive height anomaly in the Yukon and negative temperature anomaly in eastern United States is well known [2,3]. The change of half-month temperature anomaly (fig. 5D) shows that cooling occurred over the entire area east of the Continental Divide and was most intense over Illinois and Indiana.

During the latter half of January a 5-day mean High traversed an unusual path from the Great Basin northward along the western slopes of the Rocky Mountains through Alaska. The track of the High center has been plotted on the 15-day mean 700-mb. chart for January 16–30 (fig. 5B), during which period the mean ridge over the Rockies was exceptionally strong. It is noteworthy that the center followed closely the sharp ridge, and the High could be traced clearly on 5-day mean maps (prepared three times a week) from January 14 to February 4.

3. MONTHLY CIRCULATION AND TEMPERATURE PATTERNS

The most intense anomaly of the 30-day mean circulation at 700 mb. was centered in the extensive negative area in the eastern Pacific (fig. 6), associated with southeastward displacement from normal of the Aleutian Low. In the center, about 700 miles south of the Alaskan Peninsula, 700-mb. heights averaged 470 feet below normal and sea level pressures (fig. 7) 20 mb. below normal.

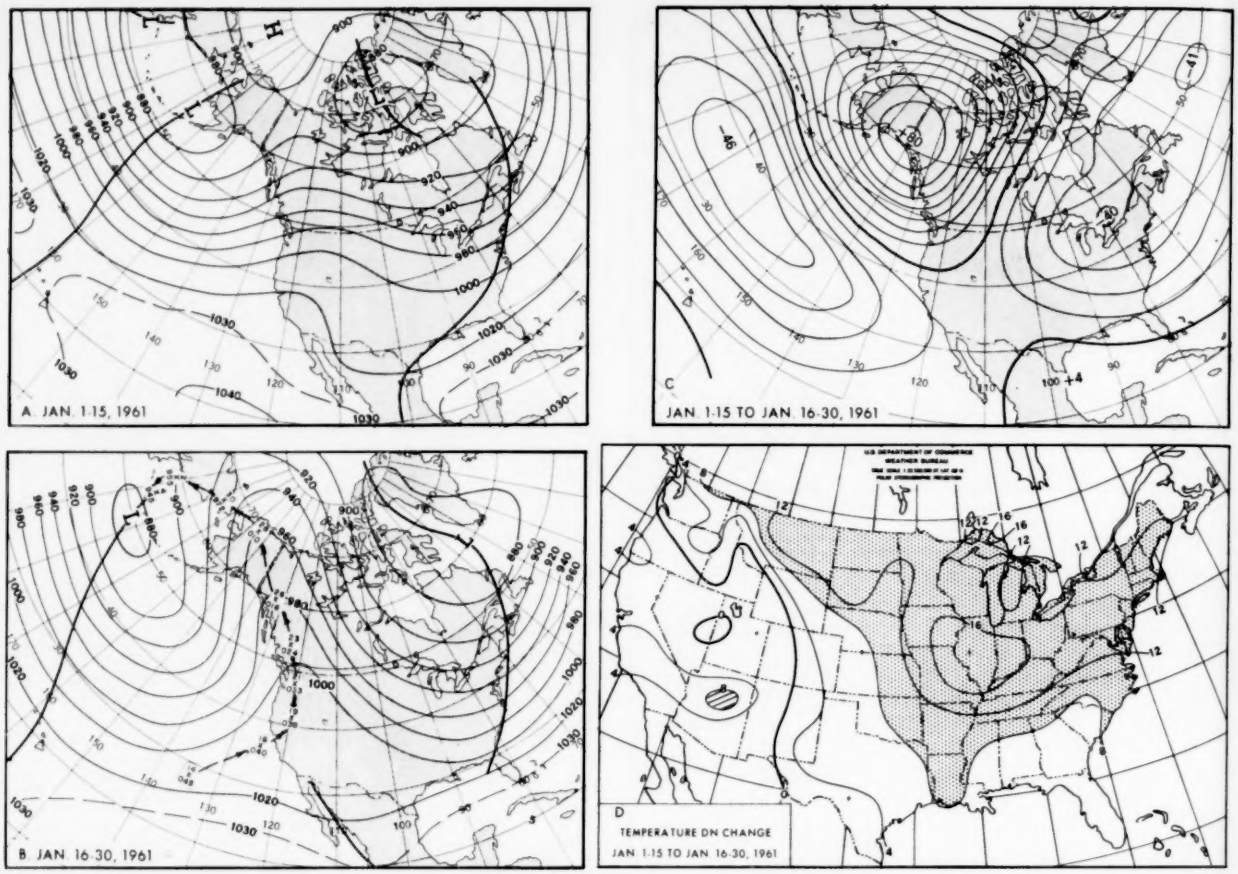

FIGURE 5.—(A) Mean 700-mb. contours (tens of feet) for January 1–15, 1961 and (B) January 16–30, 1961. Note amplification from (A) to (B) and path of a 5-day mean High over western North America from January 14 to February 4 in (B). Middle day of period is plotted above position and central intensity (in tens of feet) below. (C) Changes of 700-mb. height (tens of feet) (January 16–30 minus 1–15). Rises over the Yukon contributed to falling temperature anomalies in the United States shown in (D), the temperature anomaly change (°F.) for same periods as (C).

Progressively lesser anomalies appeared downstream, in the ridge favored by climatology over the northern Rockies, in the trough along the east coast from the Maritime Provinces southward, and in the Azores High.

Blocking, as it is represented by positive height anomalies centered north of negative anomaly centers or channels, occurred in the Davis Strait area and over the East Siberian and Beaufort Seas. The Davis Strait region has been the seat of positive anomaly centers in most Januarys since 1954. Blocking is implicit in the spreading of the mean contours over Europe, though the anomaly pattern there indicates that the condition was neither well-organized nor strong. However, the axis of maximum average wind speed at the 700-mb. level was diverted southward from its usual path into central Europe (fig. 8). Southward displacement also occurred in the eastern Pacific, eastern United States, and western Atlantic Ocean.

A secondary maximum of mean wind speed from the Arctic Basin southward through western Canada marked approximately the principal path of daily Highs (fig. 9A). These Highs were instrumental in transporting cold air into the eastern States in the latter half of the month. During the warm portion, until around the 19th, all the Arctic Highs moved eastward between Hudson Bay and the Great Lakes. Subsequently the Highs plunged southward across the Great Plains and then followed the mean axis of maximum wind speed (fig. 8) eastward into the Atlantic. In spite of the abnormality of the upper-level circulation, it is noteworthy that both of these anticyclone paths are indicated as principal tracks for January by Klein [4].

Although there was considerable variability within the month, temperature anomalies over the contiguous United States (fig. 10) did not change greatly from December. The usual test for persistence (Namias [5]) showed 85

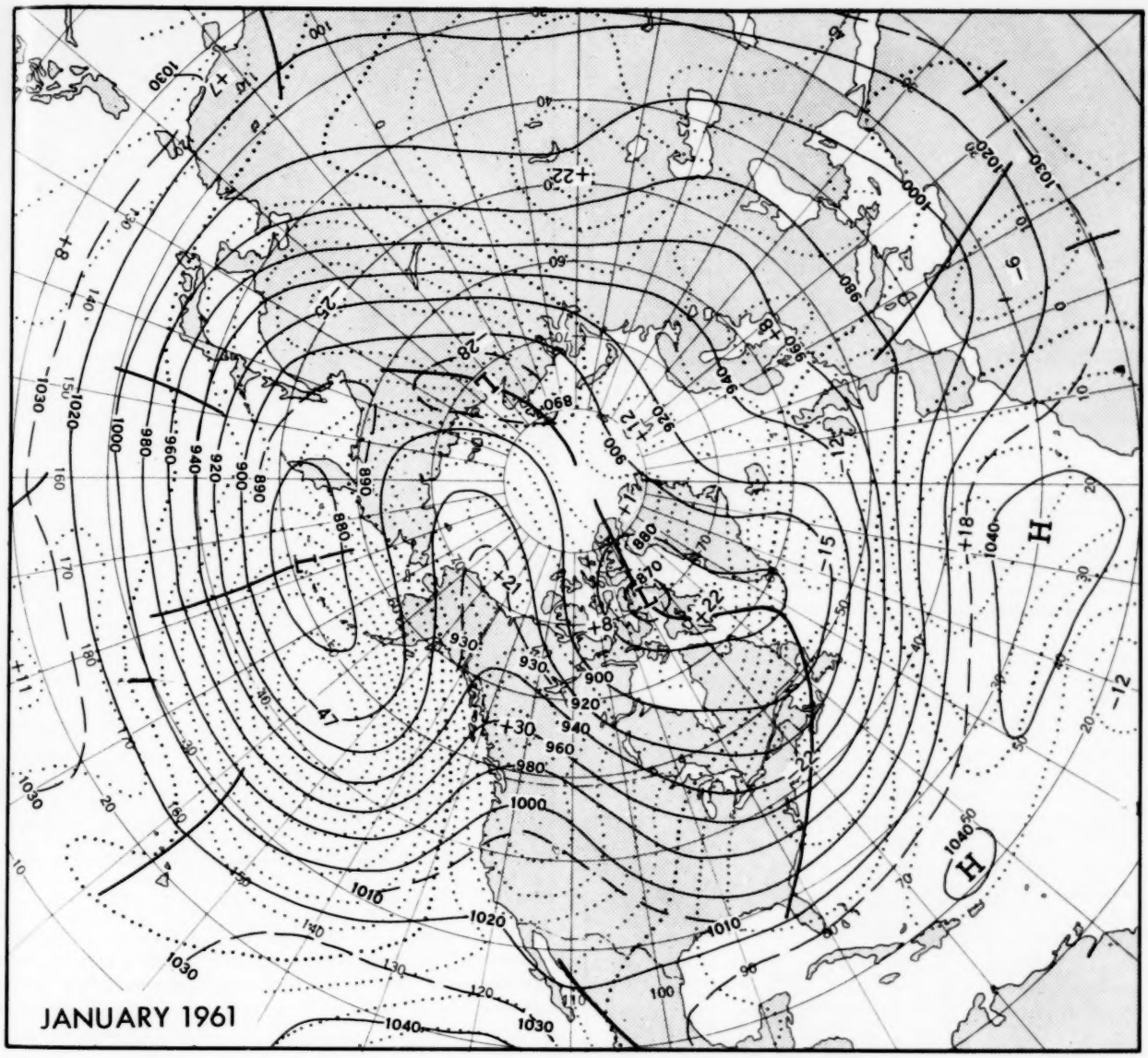

FIGURE 6.—Mean 700-mb. contours (solid) and departures from normal (dotted), both in tens of feet, for January 1961. Greatest anomaly was located in the eastern Pacific. Ridges and troughs were progressively weaker going downstream.

percent zero or one class change (out of five classes), which is high compared to the expected 71 percent. During January temperature persistence was highest over the West and the South, where changes in the circulation (fig. 5C) were not extensive. One new record for January cold was established, at Hartford, Conn., and several new marks were set for warmth in southern California. Stations listing record high averages were Blue Canyon, Burbank, Los Angeles (city office), and San Diego. These stations were in the region of warm downslope winds, locally called Santa Ana, which blow when the Great Basin High is strong at sea level. The mean sea level pressure distribution of January (fig. 7), with pressures 5 mb. higher than normal over the Great Basin, was ideal for the generation of these warm winds. In other western regions temperatures were generally warmer than normal under the influence of the persistent mean ridge.

4. PRECIPITATION

It has been mentioned that the interior of the contiguous United States was extremely dry in January. Figure 11,

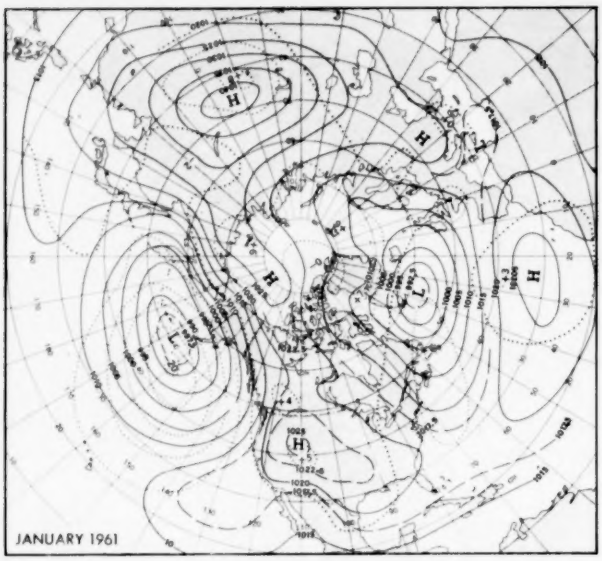

FIGURE 7.—Mean sea level isobars (solid) and departures from normal (dotted), (both in millibars) for January 1961. Intermediate isobars are dashed. Pressures were 20 mb. lower than normal south of Alaska.

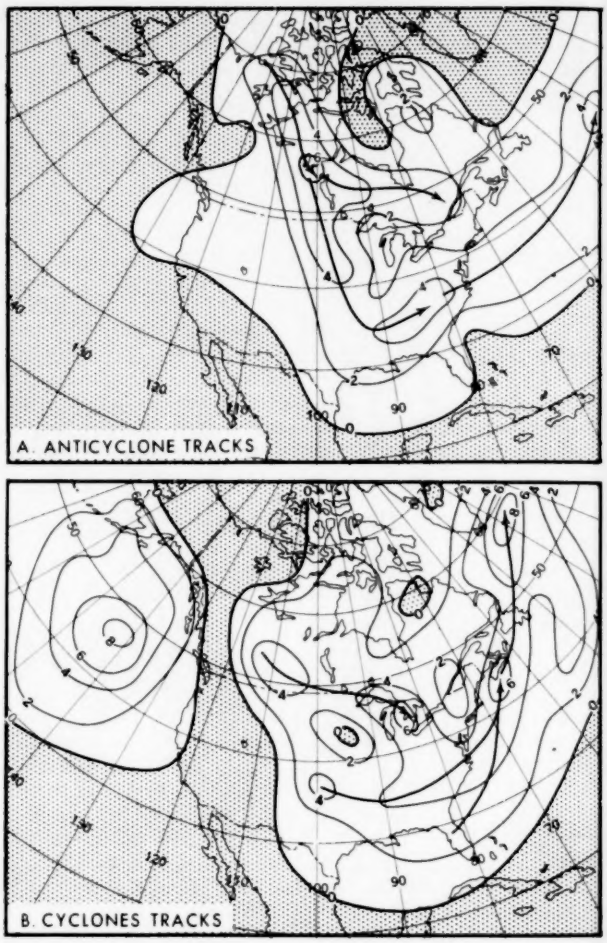

FIGURE 9.—(A) Frequency of daily anticyclone passages and (B) cyclone passages (within equal area boxes of 66,000 nautical mi.^{2}) during January 1961. Arctic Highs were diverted toward James Bay during first 20 days of month, but continued southward through Great Plains thereafter. Areas of zero frequency are shaded.

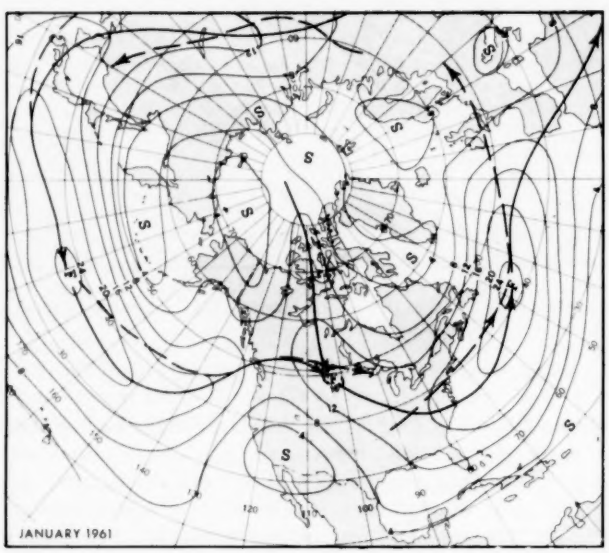

FIGURE 8.—Mean isotachs (in meters per second) of 700-mb. wind speed during January 1961. Solid arrows indicate observed axis of maximum wind speed, and dashed arrows the normal. Secondary maximum approximated principal path of Arctic High from the Polar Basin across western Canada into central United States (fig. 9A).

showing the percent of normal monthly precipitation, illustrates the large extent of the area reporting less than normal amounts. In addition to the broken records of long standing listed in table 1, there were numerous reports of "driest January" for shorter periods. Apparently the strong ridge over western North America precluded extensive upward motion and flow of appreciable moisture from the Gulf of Mexico or Pacific Ocean. Certainly no daily cyclones passed through the ridge at sea level (see fig. 9B). Several Lows of the Alberta type migrated eastward into the Great Lakes region, but Alberta Lows are typically dry.

Another group of sea level cyclones originated in Kansas or the Texas Panhandle. These too were dry initially,

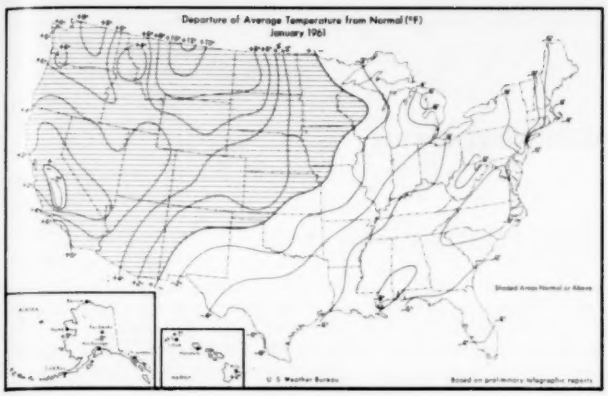
Departure of Average Temperature from Normal (°F)
January 1961
Shaded Areas Normal or Above
U. S. Weather Bureau
Based on preliminary telegraphic reports

FIGURE 10.—Departure of average temperature (°F.) from normal for January 1961 (from [6]). Hatching indicates areas of above normal temperatures.

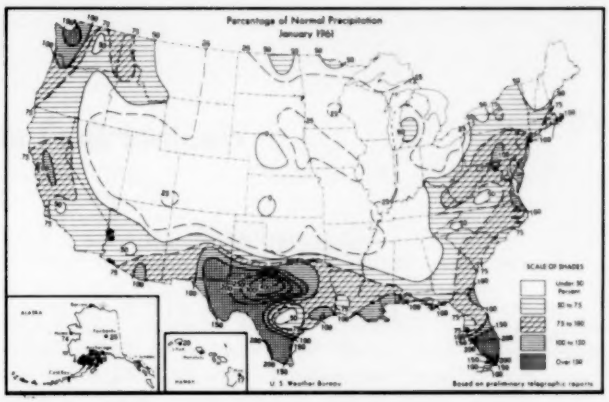

FIGURE 11.—Percentage of normal precipitation for January 1961. The month was extremely dry over most of the interior of the United States (from [6]).

in the lee of the Divide, but produced precipitation farther eastward when moisture entered the systems from the Gulf of Mexico. This group of Lows triggered the intense developments off the Atlantic coast described in section 2. Precipitation totals in the region affected by these storms averaged less than the January normal amounts except for a small area in the central Appalachians and a narrow strip along the coast from Cape Hatteras to Long Island. Snowfall was greater than normal over a larger area. Harrisburg, Pa., reported 34 inches, a new January record. At Akron, Ohio, snowfall was twice the normal, but its water content was very low and total monthly precipation was the lowest on record.

In central Texas precipitation amounts were as much as 400 percent of normal. Abilene and Waco reported the wettest January on record with 3.99 inches and 5.83 inches, respectively. There the precipitation was associated with over-running Gulf air during the passage of upper-level Lows or troughs across the Southwest, none of which was reflected appreciably in the daily sea level pressure patterns over Texas.

REFERENCES

1. R. H. Gelhard, "The Weather and Circulation of December 1960—An Unusually Cold Month in the United States," *Monthly Weather Review*, vol. 89, No. 3, March 1961, pp. 109–114.

2. D. E. Martin and H. F. Hawkins, Jr., "Forecasting the Weather—The Relationship of Temperature and Circulation Aloft," *Weatherwise*, vol. 3, Nos. 1–6, 1950, pp. 16–19, 40–43, 65–67, 89–92, 113–116, 138–141.

3. W. H. Klein, B. M. Lewis, and I. Enger, "Objective Prediction of Five-Day Mean Temperatures During Winter," *Journal of Meteorology*, vol. 16, No. 6, Dec. 1959, pp. 672–682.

4. W. H. Klein, "Principal Tracks and Mean Frequencies of Cyclones and Anticyclones in the Northern Hemisphere," *Research Paper* No. 40, U.S. Weather Bureau, 1957, 60 pp.

5. J. Namias, "The Annual Course of Month-to-Month Persistence in Climatic Anomalies," *Bulletin of the American Meteorological Society*, vol. 33, No. 7, Sept. 1952, pp. 279–285, and an unpublished extension through 1954.

6. U.S. Weather Bureau, *Weekly Weather and Crop Bulletin, National Summary*, vol. XLVIII, Nos. 2–6, Jan. 9, 16, 23, 30 and Feb. 6, 1961.

Weather Bureau Technical News

SPECIAL SLIDE RULE FOR COMPUTING EVAPOTRANSPIRATION

In response to the need for a rapid and accurate method of making daily computations of evapotranspiration from forage crops, a special slide rule has been developed by L. T. Pierce, Weather Bureau State Climatologist in Columbus, Ohio, and G. H. Snyder, Student Trainee in 1959 and 1960 at the Weather Bureau Office in Columbus. Use of this special rule, which incorporates a moderately complex empirical formula, has cut the time consumed in making numerous daily calculations by at least 50 percent of that formerly required when using a conventional slide rule or desk calculator. At the same time it has reduced the chance of error and eye strain from constant reference to tables.

This particular slide rule was designed for use in computing "actual" evapotranspiration from established meadow crops in Ohio and adjacent areas through use only of the commonly available daily temperature and rainfall data. It is intended for current use as a device for keeping track of changes in soil moisture, and also for reconstructing the probable moisture conditions prevailing in past years. An adaptation of the same type of empirical formula is now being developed for use with other common crops such as corn and wheat; and computations for these crops can be made on the same slide rule by substituting appropriate scales. Other workers in meteorology and related fields might well find this kind of tool very useful for making routine computations involving empirical formulae. In several respects, the special slide rule is preferable to the commonly-used nomogram, especially when large numbers of computations are required.

A full description of this rule, with particular emphasis on the procedures employed in its development, is given in a paper by L. T. Pierce and G. H. Snyder, "Development and Use of a Special Slide Rule for Computing Meadow Evapotranspiration," which is available as a Weather Bureau "printed manuscript" from the Publications Section, U.S. Weather Bureau, Washington 25, D.C. This paper, which contains full-size scales for use in constructing a duplicate of the original rule, is a "how-to-do-it" type of presentation that makes it relatively easy to adapt the procedures to other uses.

Suggestions for Authors

Articles are accepted for the *Monthly Weather Review* with the understanding that they have not been published or accepted for publication elsewhere.

Two copies of the *manuscript* should be submitted. All copy, including footnotes, references, tables, and captions for figures, should be double spaced with margins of at least 1 inch on sides, top, and bottom. Some inked corrections are acceptable, but pages with major changes should be retyped. The style of capitalization, abbreviation, etc., used in the *Review* is governed by the rules set down in the Government Printing Office *Style Manual*.

An *abstract* should be supplied with all but the briefest of papers. It should cover, in as concise a manner as possible, the main purpose and subject matter of the paper and indicate briefly the principal conclusions. One paragraph is usually sufficient.

Tables should be typed, each on a separate page, with a title provided. They should be numbered consecutively in arabic numerals.

In *equations* conventional symbols in accordance with the American Standards Association Letter Symbols for Meteorology should be used. If equations are written into the manuscript in longhand, dubious-looking symbols should be identified with a penciled note.

References should be listed on a separate sheet numbered in the order in which they occur in the text; or, if there are more than 10, in alphabetical order according to author. The listing should include author, title, and source (if the source is a magazine, the volume, number, month, year, and complete page numbers should be listed; if the source is a book, the publisher, place and date of publication, and the page numbers of the reference). If reference is made to a self-contained publication, the author, title, publisher, place of publication, and date should be given. Within the text, references should be indicated by arabic numbers in brackets to correspond to the numbered list.

Footnotes should be numbered consecutively in arabic numerals and indicated in the text by superscripts. Each should be typed at the bottom of the page on which the footnote reference occurs.

Illustrations.—A list of captions for the illustrations should be typed (double spaced) on a separate sheet. Every illustration should have an explanatory caption. Number each illustration in the margin or on the back outside the image area. To fit into the *Review* page, illustrations must take a reduction to 3½ by 9 inches (column size) or 7½ by 9 inches (page size). Map bases should show only political and continental boundaries and latitude and longitude lines, unless data are to be plotted, when station circles will also be needed. Usually the less unnecessary detail in the background the better will be the result from the standpoint of clear reproduction.

Line drawings and graphs should also be uncluttered with fine background grids unless the graph demands very close reading. Lines should be even and black, lettering legible, symbols distinctive, and both lettering and symbols large enough to maintain their legibility under the necessary reduction. If reproductions of line drawings are submitted because of the large size of the original, they must be extremely clear. Mimeographed copies or "photocopy" types of reproduction are not satisfactory.

Photographs should be sharp and clear, with a glossy surface. Bear in mind that marks from paper clips or writing across the back will show up in the reproduction. Drawings and photographs should be protected with cardboard and mailed flat.

Publication of Weather Notes

Many years ago the *Monthly Weather Review* published detailed eye-witness accounts of exceptional storms. These accounts both enrich the meteorologist's knowledge of storms and provide him with particular details that cannot be found elsewhere. Because such information bears directly upon questions the meteorologist must attempt to answer about weather phenomena (for example, the identification of storms as tornadoes), and because the information has potential value in both the research and service programs of the Weather Bureau, publication of eye-witness accounts and brief analyses of exceptional storms and other meteorological phenomena was resumed in the April 1955 issue. They appear from time to time under the heading "Weather Notes".

Contributions to these "Notes" are invited from readers of the Review. There is no limitation placed on length of description but it is expected that most will be short accounts. Any weather peculiarities, whether storms or other phenomena, are acceptable subject matter. Material should be addressed to Editor, Monthly Weather Review, U.S. Weather Bureau, Washington 25, D.C.

U.S. GOVERNMENT PRINTING OFFICE: 1961